Universidade Federal Fluminense

Instituto de Geociências

Programa de Pós-Graduação em Dinâmica dos Oceanos e da Terra

SABRINA PINTO RAMOS

Amazon Coastal Sediments Record the 21st-Century Shift of Global Mercury Emissions to the Tropics

Niterói, RJ

2026

SABRINA PINTO RAMOS

Amazon Coastal Sediments Record the 21st-Century Shift of Global Mercury Emissions to the Tropics

Dissertação submetida ao Programa de Pós-Graduação em Dinâmica dos Oceanos e da Terra, Universidade Federal Fluminense, como requisito parcial para obtenção do grau de Mestre.

Orientadora:
Dr. ª Ana Luiza Spadano Albuquerque

Coorientador:
Dr. º Emmanoel Vieira da Silva-Filho

Dr. º Thiago Figueiredo

Niterói, RJ
2026

Ficha catalográfica automática - SDC/BIG
Gerada com informações fornecidas pelo autor

R175a Ramos, Sabrina Pinto
Amazon Coastal Sediments Record the 21st-Century Shift of Global Mercury Emissions to the Tropics / Sabrina Pinto Ramos. - 2026.
50 f.: il.

Orientador: Ana Luiza Spadano Albuquerque.
Coorientador: Emmanoel Vieira Da Silva-Filho.
Dissertação (mestrado)-Universidade Federal Fluminense, Instituto de Geociências, Niterói, 2026.

1. Mercury accumulation. 2. Amazon Continental Shelf. 3. Sedimentary record. 4. Tropical river-ocean interface. 5. Produção intelectual. I. Spadano Albuquerque, Ana Luiza, orientadora. II. Vieira Da Silva-Filho, Emmanoel, coorientador. III. Universidade Federal Fluminense. Instituto de Geociências. IV. Título.

CDD - XXX

Bibliotecário responsável: Debora do Nascimento - CRB7/6368

SABRINA PINTO RAMOS

Amazon Coastal Sediments Record the 21st-Century Shift of Global Mercury Emissions to the Tropics

Dissertação submetida ao Programa de Pós-Graduação em Dinâmica dos Oceanos e da Terra, Universidade Federal Fluminense, como requisito parcial para obtenção do grau de Mestre.

Área de concentração: Geociências

Aprovada em 04 de fevereiro de 2026

BANCA EXAMINADORA

_____

Prof. Ana Luiza Spadano Albuquerque, Dr. (Orientador)
Universidade Federal Fluminense

_____

Prof. Emmanoel Vieira da Silva Filho, Dr. (Coorientador)
Universidade Federal Fluminense

_____

Thiago de Souza Figueiredo, Dr. (Coorientador)
Universidade Federal Fluminense

_____

Prof. Vinícius Tavares Kütter, Dr.
Universidade Federal do Pará

_____

João Marcelo Ballalai, Dr.
Universidade Federal Fluminense

AKNOWLEGMENTS

To all the energies and forces that guide me toward a kind and gentle path. I never walk alone.

To my mother by heart, Neriane, my greatest pillar and best friend. To Carlos, Vicente, Pérola, Jucilene, Leni, Weiber, João Paulo, and Johanna. To my family, who, with love and dedication, has always supported my achievements and goals. You will always be the strongest foundation I have.

To my soul sisters, Carliane, Emilly, Patrícia, Carolina, and Luanna. I am grateful for showing me a form of love that goes beyond blood. I will forever be thankful to the heavens for blessing me with your friendship.

To Nico and Mauro Arthur for your shining friendship and affection throughout all these years.

To my lover, Arthur Lebelein, who holds my hand every day and, through your calm and gentle love, supported me in every single line of this work. You bring color to my days.

To Iara and Daniel, for being part of my daily life. Living with you and calling you my friends brings me a happiness beyond words.

To my advisor, Ana Luiza, a source of inspiration, for trusting me with this project even before truly knowing me. Every piece of constructive criticism was absolutely essential to my growth. Thank you for believing in my potential.

To Emmanoel Vieira, who was crucial to this research, thank you for being a reference in mercury studies and for your willingness to help whenever needed.

To Igor Venâncio, Thiago Figueiredo, and André Belém, for their support with interpretations, statistical analyses, and graphic creation.

To Vinicius, for believing in me since my undergraduate years and for giving me the opportunity to get to know the LOOP.

To LOOP, P2L, and LaGen, for providing not only a well-equipped environment that enabled the execution of this project, but also for the dedicated and caring team that was always willing to help. In particular, I thank Raissa, Ana Chacon, Luiza, Aline, Leandro, Diego, Wladimir, Giovanna, and Thiago.

To Thaís Peccini, for starting this work alongside me and for being a constant source of friendship and support.

To AMARYLLIS expedition for the viability to develop this study.

To CAPES, for the scholarship.

To Universidade Federal Fluminense, Instituto de Geociências and PPGDOT for all structure.

Reaching this point is a powerful reminder that dreams require a great deal of courage. Sometimes, all you need is to go to a new place, where you know no one, and become Master of science.

"Science, my boy, is made up of mistakes, but they are mistakes which it is useful to make."

Julio Verne, Journey to the Center of the Earth.

ABSTRACT

Mercury (Hg) biogeochemical cycles are undergoing a profound reorganization as anthropogenic emission sources shift from industrialized regions of the Global North toward rapidly developing tropical systems in the Global South. However, empirical sedimentary evidence documenting this transition in major tropical river–ocean interfaces remain limited. Here, we reconstruct 107-year Hg accumulation record (1916-2023) at the Amazon River mouth, the world's largest fluvial–marine system, using a high-resolution ^{21}Pb-geochronology in a sediment core to disentangle global atmospheric forcing from regional anthropogenic inputs. The record reveals a pronounced acceleration in Hg accumulation beginning in the mid-20th century, with Hg fluxes increasing approximately ninefold from ~25 ng cm $^{-2}$ yr $^{-1}$ (pre-1990s) to ~230 ng cm $^{-2}$ yr $^{-1}$ in recent decades). Although long-term Hg variability broadly covaries with global anthropogenic atmospheric emission inventories, a marked divergence after ~1975 indicates the emergence of a dominant regional signal. Statistical breakpoint analyses identify a critical regime shift coincident with the rapid expansion of artisanal and small-scale gold mining and intensified deforestation across the Amazon Basin. The analysis of excess Hg, together with its strong co-variation with lithogenic elements, demonstrates that erosional mobilization of legacy soil Hg and direct mining-related inputs now outweigh long-range atmospheric deposition. These findings provide the first century-scale sedimentary evidence that the Amazon River mouth has transitioned from recording predominantly global Hg emissions to functioning as a net regional Hg accumulator. This positions tropical river mouths as critical sentinels for tracking anthropogenic mercury redistribution. Our results underscore the urgent need to incorporate land-use-driven Hg mobilization into global emission inventories and the Minamata Convention monitoring frameworks.

Keywords: Mercury accumulation; Amazon Continental Shelf; Sedimentary record; Tropical river–ocean interface.

RESUMO

Os ciclos biogeoquímicos do mercúrio (Hg) estão passando por uma profunda reorganização à medida que as fontes de emissão antropogênica se deslocam de regiões industrializadas do Norte Global para sistemas tropicais em rápido desenvolvimento no Sul Global; no entanto, evidências sedimentares empíricas que documentem essa transição em grandes interfaces rio–oceano tropicais ainda são limitadas. Neste estudo, reconstruímos 107 anos de acumulação de Hg (1916–2023) na foz do rio Amazonas, o maior sistema fluvial–marinho do mundo, utilizando uma geocronologia de alta resolução baseada em ^{210}Pb aplicada a um testemunho sedimentar, com o objetivo de distinguir o forçamento atmosférico global dos aportes antropogênicos regionais. O registro revela uma acentuada aceleração na acumulação de Hg a partir de meados do século XX, com os fluxos de Hg aumentando aproximadamente nove vezes após o início dos anos 2000 (de ~25 ng.cm^{-2}.ano^{-1} antes da década de 1990 para ~230 ng.cm^{-2}.ano^{-1} nas décadas recentes). Embora a variabilidade à longo prazo do Hg covarie amplamente com inventários globais de emissões atmosféricas antropogênicas, uma divergência marcante após ~1975 indica o surgimento de um sinal regional dominante. Análises estatísticas de breakpoints identificam uma mudança crítica de regime coincidente com a rápida expansão da Mineração Artesanal e de Pequena escala de Ouro e com a intensificação do desmatamento em toda a bacia amazônica. Os excessos de Hg juntamente com a covariação com elementos litogênicos, demonstram que a mobilização erosiva do histórico de Hg nos solos, assim como os aportes diretos associados à mineração passaram a superar a deposição atmosférica de longa distância. Esses resultados fornecem a primeira evidência sedimentar em escala secular de que a foz do rio Amazonas deixou de registrar predominantemente emissões globais de Hg e passou a funcionar como um sistema regional ativo de mercúrio, posicionando as desembocaduras de grandes rios tropicais como sentinelas críticas para o monitoramento da redistribuição antropogênica de Hg. Nossos resultados ressaltam a necessidade urgente de incorporar a mobilização de Hg induzida por mudanças no uso da terra nos inventários globais de emissões e nos marcos de monitoramento da Convenção de Minamata.

Palavras-chave: Acumulação de mercúrio; Plataforma Continental Amazônica; Registro sedimentar; Interface rios Tropicais-oceano.

LIST OF FIGURES

Figure 1: Study area and core locations. (A) Regional map showing the Amazon River mouth and the northwestern Atlantic continental margin. The Amazon River plume is represented schematically. (B) Detail of the sampling area on the Amazon Continental Shelf. Core MD23-3660Q (station S10, red square) was retrieved from the inner shelf (70 m water depth) under the direct influence of the river plume. Cores MD23-3652Q and MD23-3653 (station S6, blue triangle) were collected from the continental slope (2518 m water depth) and are used to establish a regional background. Bathymetric contours are shown in meters. The map was created using [e.g., Ocean Data View, QGIS, or Generic Mapping Tools]. 19

Figure 2: ^{210}Pb-based chronology and accumulation history of core MD23-3660Q. **(A)** Downcore profile of unsupported ^{21} Pb ^{21} Pbex) showing the characteristic exponential decay used for geochronology. **(B)** Age–depth model derived from the Constant Rate of Supply (CRS) model. The dashed segment represents the conservative linear extrapolation applied below the depth of detectable ^{21} Pbex; these ages are used for stratigraphic context only. **(C)** Temporal variability of sedimentation rates over the past century, illustrating the non-steady-state deposition regime of the Amazon Continental Shelf. 25

Figure 3: Mercury concentration and depositional flux over the last century in core MD23-3660Q. **(A)** Downcore Hg concentration profile (ng g^{-1}) compared to the natural interglacial background range (shaded area) derived from offshore reference cores MD23-3652Q and MD23-3653. All concentrations in the shelf core exceed pre-anthropogenic background levels. **(B)** Historical Hg depositional flux (ng cm^{-2} yr^{-1}), calculated as the product of Hg concentrations, sediment accumulation rate, and dry bulk density. The flux record highlights changes in the actual mass of Hg buried per unit area per year, providing a direct measure of anthropogenic forcing distinct from concentration variations driven by sediment dilution. 28

Figure 4: Disentangling global and regional sources. **(A)** Z-score standardized records of sedimentary Hg in core MD23-3660Q (local, blue) and Global Anthropogenic Atmospheric

Emissions (GAAE, global, orange). The parallel long-term rise (pre-1990s) and subsequent divergence are visually apparent. **(B)** Mercury excess (Hg_{exc}), calculated as the difference between standardized records (local - global). Positive (Hg_{exc}) values (shaded) indicate periods when Hg accumulation on the Amazon shelf exceeded the trajectory of global atmospheric emissions, signaling the growing dominance of regional anthropogenic sources. The transition to sustained positive values after the mid-1990s marks a fundamental shift in the Hg source regime. 31

Figure 5: Statistical identification of depositional regime shifts. Early Warning Signals (EWS) analysis applied to Hg_{exc} time series, showing rolling-window variance. The horizontal dashed line indicates the 90th percentile significance threshold. Variance peaks exceeding this threshold identify two major breakpoints (~1995, ~ 2004), marked by vertical lines. These statistically derived breakpoints objectively validate the transition between the three Hg source regimes (global, transitional, regional) identified in the record, corroborating the shift from atmospheric to land-use dominated Hg forcing. 31

Figure 6: Decoupling of mercury from bulk sediment geochemistry. (A) Principal Component Analysis (PCA) biplot for sediments with moderate anthropogenic influence. The distribution of samples and variable loadings (vectors) on the first two components (PC1, PC2) reveals a dominant geochemical gradient aligned with Hg, which clusters near the origin (weak loadings). **(B)** Direct comparison of Hg concentrations against PC1 scores confirms the lack of a predictive relationship (r=0.02, p=0.87r=0.02, p=0.87). Together, these results demonstrate that Hg accumulation is not controlled by the major lithogenic or organic components of the sediment matrix, supporting its origin from external anthropogenic inputs. 33

Figure 7: Conceptual model of mercury source transition and amplification at the Amazon River mouth. The model synthesizes the key drivers of Hg accumulation over the past century, derived from the sedimentary record of core MD23-3660Q. It depicts a temporal transition from a Global Atmospheric Regime (pre – 1990s), where Hg deposition tracked

worldwide emission trends, to a Regional Anthropogenic Regime (post – 1990s), dominated by inputs from artisanal gold mining (ASGM) and land-use change (e.g., deforestation). This regional signal is physically amplified by the Amazon's exceptionally high sediment loads and variable sedimentation rates, leading to disproportionate increases in Hg burial fluxes. The Amazon Continental Shelf functions as an integrator and a sentinel system, providing a critical sedimentary baseline for monitoring the effectiveness of global agreements like the Minamata Convention in the tropics. 41

LIST OF ABBREVIATIONS

^{210}Pb	Lead-210
$^{210}Pb_{Exc}$	Unsupported Lead-210
^{214}Bi	Bismuth-214
^{214}Pb	Lead-214
^{226}Ra	Radium-226
ACS	Amazon Continental Shelf
ASGM	Artisanal and Small-scale Gold Mining
CIC	Constant Initial Concentration
cm	centimeter
CRS	Constante Rate of Supply
ENSO	El Niño–Southern Oscillation
EWS	Early Warning Signals
$Flux_{Hg}$	Mercury Flux
g	gram
GAAE	Global Atmospheric Emissions
Hg	Mercury
Hg_{exc}	Mercury Excess
MAR	Mass Accumulation Rates
MD23-3652Q	Marion Dufresne 23-3652Q
MD23-3653	Marion Dufresne 23-3653
MD23-3660Q	Marion Dufresne 23-3660Q
Mg	Megagram
NBC	North Brazil Current
ng	Nanogram
PCA	Principal Componente Analysis
PLSR	Partial Least Square Regression
SR	Sedimentation Rate
TOC	Total Organic Carbon
XRF	X-ray Flourescence
yr	Year

Sumário

Introduction 1

Study area 3

Material and methods 4

Sediment Core and Analytical Framework 4

^{210}Pb Gamma Spectometry and Sedimentation Rates 5

Laboratory Analyses 7

Data Analysis and source attribution framework 8

Results. 10

Geochronology and sediment accumulation rates 10

Sedimentation and Mass Accumulation Rates 12

Temporal variability of Hg concentrations 12

Hg depositional fluxes 15

Global Hg Excess and Identification of Depositional Regimes 15

Geochemical associations and multivariate patterns 18

Discussion 20

From global atmospheric forcing to regional dominance in Amazonian Hg deposition 20

Sedimentation as a key amplifier of mercury accumulation at the Amazon River mouth 21

Geochemical controls and the absence of a single dominant Hg carrier phase 23

Implications for monitoring tropical Hg dynamics under the Minamata Convention 24

Conclusions 26

References 28

Introduction

The global Mercury (Hg) cycle has been fundamentally reshaped by anthropogenic activities over the past five centuries. Historical emissions, first driven by silver and gold extraction in colonial Spanish America and later by the 19th-century Gold Rush in North America, established Hg as a globally dispersed pollutant concentrated in the Northern Hemisphere (Brown, 2016; Streets et al., 2011). In the modern area, primary anthropogenic sources include fossil-fuel combustion, industrial activities, and Artisanal and Small-Scale Gold Mining (ASGM) (Corbitt et al., 2011; Qiu et al., 2025; Dastoor et al., 2022). Recent inventories, however, reveal a profound geographical shift: declining emissions in the Global North and China are now being offset by rising contributions from the Global South, particularly tropical regions undergoing rapid land-use change (Qiu et al., 2025). This reorganization underscores the critical importance of the Minamata Convention on Mercury, a landmark 2017 treaty aimed at reducing anthropogenic emissions. Yet, evaluating its effectiveness remains challenging in these very regions where observational baselines are sparse and regional Hg dynamics are poorly constrained.

In addition to direct emissions, Hg cycling is modulated by climatic variability, which influences its mobilization and sequestration over glacial-interglacial timescales through precipitation, atmospheric circulation, and organic matter dynamics (Fadina et al., 2019; Figueiredo et al., 2020). At regional scales, however, land-use disturbances such as deforestation, soil erosion, and mining can rapidly remobilize legacy Hg stored in soils, overwhelming these broader climatic controls. Consequently, sedimentary Hg records integrate multiple, interacting drivers operating across different temporal and spatial scales.

Against this backdrop of global change, the Amazon Basin emerges as a critical region. Draining 6.1 million km² and discharging over 200,000 m³/s into the Atlantic Ocean, the Amazon River exports 1.1-1.3 billion tons of sediment annually, sustaining a vast continental shelf that acts as a global biogeochemical hotspot (Oliveira and Ferreira, 2024; Carneiro and Mancini, 2023). The river functions not merely as a conduit but as an active processor of mercury, integrating atmospheric deposition, basin-scale erosion, and direct anthropogenic releases. This role is amplified because Hg strongly adsorbs onto Fe- and Al-(oxy)hydroxides and organic compounds associated with fine-grained sediments within the riverine plume (Garnier et al., 2025; Mendes et al., 2016). Subsequent physical-chemical processes, such as flocculation and hydrodynamic sorting on the shelf, ultimately determine the burial efficiency of these metal-organic complexes (Do Nascimento et al., 2025).

Despite extensive research within the Basin, a significant knowledge gap persists regarding Hg dynamics on the adjacent coastal shelf, largely due to logistical challenges (Do Nascimento et al., 2024). This gap is critical because coastal sediment archives are uniquely positioned to preserve an integrated, century-scale record of both global atmospheric signals and regionally driven continental inputs. Furthermore, the Amazon exemplifies the new epicenter of anthropogenic Hg pressure. The region is global leader in ASGM and large-scale mining (e.g., iron ore. Bauxite), activities that drive extensive land-use transformation and remobilize legacy soil Hg (ANM, 2024; Santos et al., 2023). Recent modeling indicates that deforestation itself acts as a potent anthropogenic Hg source by eroding this historical stockpile (Feinberg aet al., 2024). As a result, the Amazon is now a major hotspot for Hg emissions and re-emissions, contributing significantly to global atmospheric totals and representing the world's largest fluvial source of Hg to the ocean (Ferreira et al., 2024; Pfeiffer and Drude, 1988; Souza et al., 2025). This shift underscores a fundamental divergence from Northern Hemisphere dynamics, influenced by limited inter-hemispheric mixing and the dominance of the terrestrial vegetation sink in the South (Fisher et al., 2023).

The pressing need, therefore, is for empirical, long-term sedimentary records capable of capturing this source transition from global atmospheric to regional land-use dominance. Such records are essential to establish baselines and evaluate treaty effectiveness in tropical systems.

Here, we present the first century-scale reconstruction of Hg deposition at the Amazon River mouth using ^{21} Pb-dated sediment cores from the continental shelf. Our primary objectives are to: (1) quantify temporal trends in Hg concentration and mass accumulation rates over the past ~107 years (1916-2023); (2) identify statistical change-points in the record and correlate them with key historical drivers (ASGM expansion, deforestation acceleration); and (3) evaluate the relative contributions of global atmospheric versus local/regional sources by comparing the sedimentary Hg record with independent time series of land-cover change, ASGM activity, and climatic indices. We hypothesize that: (H1) Hg accumulation rates increased most sharply after the 1970s, coinciding with the expansion of ASGM and accelerate deforestation in the Amazon, rather than with mid-20th century industrial peaks in the Northern Hemisphere; and (H2) the temporal patterns of mercury accumulation will correlate more strongly with regional land-use metrics than with global atmospheric emission inventories, providing robust sedimentary evidence for the ongoing North-to-South transition of anthropogenic Hg emissions. By establishing this centennial baseline, we aim to position

the Amazon River mouth as a key sentinel site for monitoring tropical Hg dynamics and to provide one of the first empirical sedimentary benchmarks for evaluating the effectiveness of the Minamata Convention in a large, rapidly changing tropical system.

Study area

The Amazon River, extending approximately 6,400 km, plays a fundamental role in global cycles. With an annual mean discharge of ~ 200,000 $m^3.s^{-1}$, it generates an extensive river plume that dominates circulation and biogeochemistry across the western equatorial Atlantic Ocean (de Freitas et al., 2025; Morozov et al., 2024). This plume represents one of the world's largest river-dominated ocean margins and is a critical interface for transferring water, sediments, nutrients and contaminants from the continent to the ocean. Typically extends over the Brazilian continental shelf at depths of ~3-15m, the Amazon Continental Shelf (ACS) is characterized by intense hydrodynamics modulated by fluvial discharge, trade winds, tides, and the North Brazil Current (NBC), under a dominant semidiurnal tidal regime (de Freitas et al., 2025).

The Amazon basin contributes 16-20% of global freshwater discharge to the Atlantic Ocean, delivering large quantities of sediments and organic matter (Crizanto et al., 2024; Morozov et al., 2024). This exceptional sediment load promotes the efficient scavenging and downstream transport of particle-reactive trace metals, including mercury, to the continental shelf. Discharge variability is controlled by precipitation patterns, winds stress, storm activity, ocean circulation and tidal forcing (Morozov et al., 2024). Consequently, the magnitude and timing of sediment and contaminant delivery to the ACS are highly dynamics and sensitive to climatic and hydrological variability.

Within this system, the Amazon River and the ACS are significant zones for the transport, redistribution, and burial of Hg in marine sediments. Fine-grained particles in the river plume provide an efficient vector for Hg export, while shelf hydrodynamics regulate its lateral dispersal, resuspension and long-term accumulation. Thus, the ACS functions not merely as a depositional sink but as an active processing zone where continental Hg inputs are integrated, transformed and archived.

Anthropogenic pressures in the basin intensified markedly from the 1960's onward, driven by Brazilian federal policies promoting economic expansion and colonization (Trindade and Barbosa Filho, 2002). Although artisanal and small-scale gold mining (ASGM) has occurred since the 16th century, Hg emissions surged in the 1970's the rise of large-scale operations such as Serra Pelada (Barbosa et al., 1992; Trindade and Barbosa Filho, 2002). This period marks the onset of widespread basin-scale disturbance, with direct Hg releases from amalgamation superimposed on enhanced erosion from land-clearing. Furthermore, large-scale development projects (e.g., Carajás iron-ore complex) and associated deforestation likely enhanced the mobilization and re-emission of legacy Hg stored in soils and sediments (Lacerda, 2003; Trindade and Barbosa, 2002).

Material and methods

Sediment Core and Analytical Framework

To reconstruct the Hg depositional history, we analyzed core MD23-3660Q (3°06.278′ N, 49°23.777′ W), recovered from the ACS at a water depth of 70 m, (total length: 11.14 m). The core was collected during the 2023 AMARYLLIS Cruise aboard the R/V *Marion Dufresne*. The site lies under the direct influence of the Amazon River plume, close to the river mouth (Figure 1), a location chosen to maximize sensitivity to both atmospheric Hg deposition and riverine inputs linked to basin-scale land-use change. An age model and sedimentation rates were established using ^{210}Pb geochronology. Geochemical and sedimentological analyses, including Total Organic Carbon (TOC), grain size, X-ray Fluorescence (XRF), and mercury concentrations, were performed to reconstruct Hg deposition.

For comparison and establish a natural background, we also analyzed two deeper offshore cores from the broader region (Figure 1): core MD23-3652Q (6°39.388 N, 52°04.760 W; 2518 m depth; 10.49 m length) and CALYPSO core MD23-3653 (6°39.363 N, 52°04.745 W; 2518 m depth; 50.37 m length). These records provide a pre-anthropogenic and interglacial reference framework, essential for distinguishing recent anthropogenic enrichment from long-term natural variability.

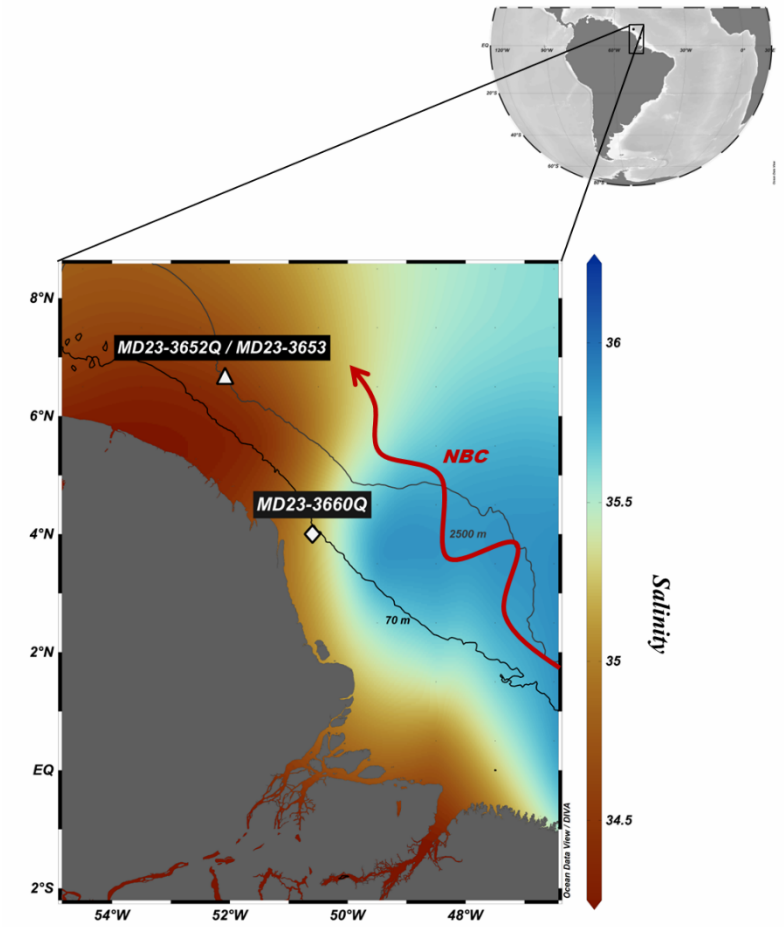

Figure 1: Study area and core locations. (A) *Regional map showing the Amazon River mouth and the northwestern Atlantic continental margin. The Amazon River plume is represented schematically. (B) Detail of the sampling area on the Amazon Continental Shelf. Core MD23-3660Q (station S10, red square) was retrieved from the inner shelf (70 m water depth) under the direct influence of the river plume. Cores MD23-3652Q and MD23-3653 (station S6, blue triangle) were collected from the continental slope (2518 m water depth) and are used to establish a regional background. Bathymetric contours are shown in meters. The map was created using [e.g., Ocean Data View, QGIS, or Generic Mapping Tools].*

^{210}Pb Gamma Spectometry and Sedimentation Rates

Sediment chronology and sedimentation rates were determined using ^{210}Pb gamma spectrometry. A total of 12 samples were analyzed by a high-resolution gamma spectrometry, using a Camberra HPGe detector (40% relative efficiency), housed in a low background lead shield and coupled to a multichannel analyzer. Each sample was counted for at least 80,000 seconds to ensure adequate counting statistics. Prior to analysis, samples were hermetically sealed for a minimum of 21 days to allow secular equilibrium between ^{226}Ra and its short-lived daughters products (^{214}Pb and ^{214}Bi). Supported ^{210}Pb activity was estimated from the measured ^{226}Ra activity, determined by averaging the gamma emissions of ^{214}Pb (295,2 and

351 keV) and ^{214}Bi (609 keV). Total ^{210}Pb activity was measured via its 46.5 keV gamma emission. Background subtraction and self-absorption corrections were applied. Detector efficiency and energy calibrations were performed using the CANMET BL-4a uranium ore reference material. Analytical uncertainties were generally below 5%, ensuring robust activity determinations. Unsupported (excess) ^{210}Pb ($^{210}Pb_{Exc}$) activities were calculated by subtracting the supported activity from the total activity.

Sediment ages and sedimentation rates were calculated using the Constant Rate of Supply (CRS) model (Appleby and Oldfield, 1978). This model assumes a constant flux of atmospheric $^{210}Pb_{Exc}$ to the sediment surface while allowing variable sediment accumulation rates. It is particularly appropriated for high-energy continental shelf environments, like the Amazon Continental Shelf, where sedimentation rates are known to vary substantially in response to hydrodynamic and fluvial forcing. In contrast, the Constant Initial Concentration (CIC) model, which assumes invariant sediment accumulation, was deemed unsuitable for this dynamic setting.

According to the CRS model, the sediment age $t(z)$ at depth z is given by:

Where $A_{(z)}$ is the cumulative unsupported ^{210}Pb inventory below depth z, A_0 is the total unsupported ^{210}Pb inventory in the core, and λ is the decay constant for ^{210}Pb ($\lambda = 0.0311$ yr^{-1}).

Applying the CRS model yielded reliable ages for the interval from 0.5 cm to 300.5 cm depth, where measurable $^{210}Pb_{exc}$ activities were detected. This interval, spanning approximately the last 100–150 years, covers the period of interest for reconstructing anthropogenic Hg deposition. Derived sedimentation rates for this section ranged from 2.48 to 13.12 cm yr ^{1}, reflecting strong temporal variability consistent with the highly dynamic depositional regime of the Amazon shelf.

Below 300.5 cm, $^{210}Pb_{exc}$ activities approached supported (background) levels, precluding direct age determination. To maintain stratigraphic continuity and provide a broader context, the age model was conservatively extrapolated linearly to ~401.5 cm depth, based on the sedimentation rate in the deepest reliably dated interval. This extrapolation extends the chronology by approximately 40 years, resulting in a continuous ~107 years

record (1916–2023). Ages below 300.5 cm are considerate qualitative estimates and were not used for calculating mass accumulation rates (MAR) or Hg depositional fluxes.

The CRS model resolved distinct sedimentation regimes with the following rates and corresponding mass accumulation rates (MAR, assuming a constant dry bulk density of 0.35 g cm-3 derived from parallel measurements):

1. **0.5–50.5 cm:** 13.12 cm yr ^{1} (MAR ≈ 2.30 g cm ^{2} yr ^{1})
2. **50.5–99.5 cm:** 3.49 cm yr ^{1} (MAR ≈ 0.61 g cm ^{2} yr ^{1})
3. **99.5–150.5 cm:** 7.58 cm yr ^{1} (MAR ≈ 1.32 g cm ^{2} yr ^{1})
4. **150.5–200.5 cm:** 3.88 cm yr ^{1} (MAR ≈ 0.68 g cm ^{2} yr ^{1})
5. **200.5–248.5 cm:** 6.62 cm yr ^{1} (MAR ≈ 1.15 g cm ^{2} yr ^{1})
6. **248.5–300.5 cm:** 2.48 cm yr ^{1} (MAR ≈ 0.43 g cm ^{2} yr ^{1})

This pronounced variability in sedimentation and accumulation rates underscores the necessity of using a chronology that accommodates non-steady-state deposition when accurately reconstructing historical contaminant fluxes on the Amazon Continental Shelf.

Laboratory Analyses

One hundred and fifty samples were collected from the CASQ core MD23-3660Q at a 4 cm resolution, providing high stratigraphic detail across the upper portion of the record. This sampling resolution was selected to capture decadal-scale variability in Hg deposition over the past century, consistent with the temporal resolution of the ^{210}Pb chronology. All samples were freeze-dried (lyophilized) and subsequently ground to a fine powder to ensure homogeneity prior to analysis.

Total Organic Carbon (TOC) was determined using a LECO CS-200 carbon analyzer. Inorganic carbon was removed by acidification with 1M HCl prior to analysis. TOC measurements were used to evaluate the potential role of organic matter as a primary carrier phase for Hg in the shelf sediments.

Grain-size distribution was determined using laser diffraction. Organic matter was first removed by repeated treatment with 10% hydrogen peroxide (H_2O_2) until the reaction ceased, minimizing particle aggregation. The treated samples were then analyzed with a Shimadzu

SALD-3101 laser diffraction particle-size analyzer, yielding the relative percentages of clay, silt and sand.

Elemental composition was determined by X-ray Fluorescence (XRF) spectrometer using an Epsilon 1 (PANalytical) spectrometer with excitation energies of 10keV and 30keV. This enabled the quantification of major lithogenic elements (Al, Fe, Ti, K, Si, Ca), which serve as proxies for detrital mineral input, sediment provenance, and potential dilution effects.

Mercury concentrations were measured using a RA-915+ mercury analyzer with a PIRO-915+ dual-chamber pyrolysis atomizer, following the methodology of Sholupov et al. (2004). This technique allows for direct determination of total Hg without chemical pre-treatment, minimizing contamination risks and losses through volatilization, while providing low detection limits (< 0.5 ng g ^{1}) and high precision. Quality assurance included the analysis of certified reference materials replicate measurements of selected samples, and routine calibration checks. Analytical precision, based on replicate analyses, was better than 5%.

Data Analysis and source attribution framework

A comprehensive data analysis framework was implemented using Python 3.10 (libraries: *Numpy*, *Pandas*, SciPy, Scikit-learn, *Seaborn*) to quantify mercury depositional fluxes, evaluate temporal trends, and distinguish regional anthropogenic inputs from global atmospheric forcing. The strategy was designed to combine physically based calculations with exploratory and confirmatory statistical approaches, thereby avoiding over-reliance on any single method.

Mercury depositional fluxes ($Flux_{Hg}$, ng cm^{-2} yr^{-1}) were reconstructed by combining Hg concentrations, sedimentation rates (SR) from the CRS ^{210}Pb chronology, and a constant dry bulk density (ρ = 0.175 g/cm^{3}). Flux and mass accumulation rate (MAR) calculations were restricted to the upper 300.5 cm of the core, the interval directly constrained by ^{210}Pb dating, to avoid uncertainties associated with age extrapolation. $Flux_{Hg}$ was calculated as:

$$\mathbf{Flux_{Hg}}\ (\text{ng cm}^{-2}\ \text{yr}^{-1}) = \text{SR (cm yr}^{-1}) \times \rho\ (\text{g cm}^{-3}) \times [\text{Hg}]\ (\text{ng g}^{-1})$$

To assess the relative influence of global versus regional Hg sources, the local sedimentary Hg record was compared to an annual composite record of Global Anthropogenic

Atmospheric Emissions (GAAE). The GAAE record was constructed by temporally interpolating and merging historical emission inventories from Streets et al. (2011) and EDGAR v8.1. Both time series were standardized (z-score normalization) to isolate relative temporal deviations. Mercury excess (Hg_{exc}) was then defined as:

$$\mathbf{Hg}_{\mathbf{excec}}(z) = z\,(\mathbf{Hg}_{\mathbf{local}}) - z\,(\mathbf{Hg}_{\mathbf{global}})$$

Where z denotes the z-score. Positive Hg_{exc} values indicate periods when local Hg accumulation outpaces the global atmospheric trend, suggesting dominant regional forcing, while negative values imply relative deficits or dilution.

Temporal Breakpoint Analysis. To identify structural changes in the Hg accumulation record, an Early Warning Signals (EWS) approach was applied using rolling-window variance. Statistically meaningful regime shifts were identified only where variance peaks exceeded the 90th percentile of the distribution, minimizing false-positive detection. These breakpoints were used to define distinct depositional phases rather than to fit predictive models.

Correlation Analysis. Pairwise relationships were evaluated using Pearson correlation (linear association), Spearman´s rank correlation (monotonic association), and Kendall´s τ (rank concordance). The multi-metric approach ensures robustness to non-linearities and outliers.

Multivariate Geochemical Analysis. A multivariate dataset comprising 15 variables (major/minor elements, TOC, grain-size fractions) was analyzed to explore geochemical controls on Hg. First, unsupervised K-means clustering was applied for pattern recognition and data stratification. The optimal number of clusters was determined using the elbow method and silhouette score analysis. Subsequently, Principal Component Analysis (PCA) was applied to the subset of data representing moderate anthropogenic influence to identify dominant compositional gradients. Interpretation focused on the covariance structure (component loadings) rather than variance maximization alone.

Predictive Modeling. To test whether Hg variability could be explained solely by lithogenic factors, predictive models (Random Forest and Partial Least Squares Regression, PLSR) were implemented using k-fold cross-validation. Model performance was explicitly evaluated to assess predictability. Poor performance was interpreted not as a methodological

failure, but as positive evidence that Hg dynamics are governed by multidimensional controls beyond the measured geogenic proxies.

Results

Geochronology and sediment accumulation rates

The unsupported ^{210}Pb ($^{210}Pb_{exc}$) activity profile in core MD23-3660Q shows a well-defined exponential decrease with depth (Figure 2), confirming continuous sediment accumulation and validating the use of ^{210}Pb geochronology for the upper sequence. The Constant Rate of Supply (CRS) model was therefore applied to establish the age-depth relationship.

Application of the CRS model yielded a reliable chronology for the interval from 0.5 and 300.5 cm depth, where detectable $^{210}Pb_{exc}$ activity was present. This interval represents approximately 107 years of deposition, spanning from 1916 to 2023. Derived sedimentation rates within this well-constrained zone were highly variable, ranging from 2.48 to 13.12 cm yr^{-1}.

Below 300.5 cm, $^{210}Pb_{exc}$ activities decayed to near-background levels, precluding direct age determination. To provide a continuous stratigraphic context, the age model was conservatively extrapolated linearly to ~401.5 cm depth. All subsequent calculations of mercury flux and mass accumulation rates were restricted to the reliably dated upper 300.5 cm, excluding the extrapolated section.

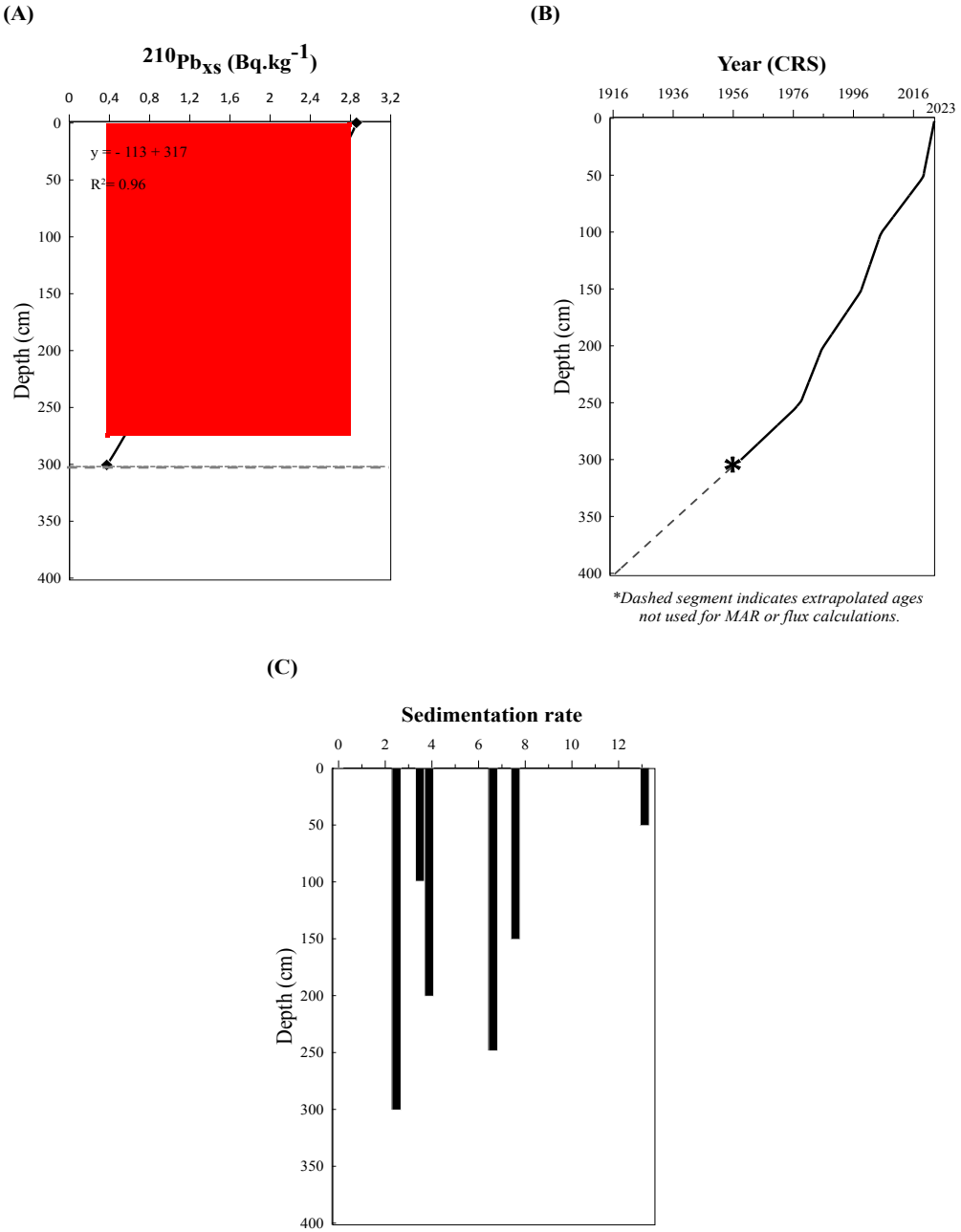

Figure 2: ^{210}Pb-based chronology and accumulation history of core MD23-3660Q. **(A)** Downcore profile of unsupported ^{21} Pb ^{21} Pbex) showing the characteristic exponential decay used for geochronology. **(B)** Age–depth model derived from the *Constant Rate of Supply (*CRS) model. The dashed segment represents the conservative linear extrapolation applied below the depth of detectable ^{21} *Pbex; these* ages are used for stratigraphic context only. **(C)** Temporal variability of sedimentation rates over the past century, illustrating the non-steady-state deposition regime of the Amazon Continental Shelf.

Sedimentation and Mass Accumulation Rates

Sedimentation rates derived from the CRS chronology reveal substantial, non-steady-state deposition over the past century (Figure 2C). Rates varied markedly between adjacent core intervals: 0.5–50.5 cm: 13.12 cm yr^{-1}; 50.5–99.5 cm: 3.49 $cm.yr^{-1}$;, 99.5–150.5 cm: 7.58 $cm.yr^{-1}$; 150.5–200.5 cm: 3.88.cm yr^{-1}; 200.5–248.5 cm: 6.62 $cm.yr^{-1}$; and 248.5–300.5 cm: 2.48 $cm.yr^{-1}$.

This pronounced temporal variability, spanning an order of magnitude, underscores the highly dynamic sedimentary regime of the Amazon Continental Shelf (ACS)

Corresponding mass accumulation rates (MAR) ranged from 0.43 to 2.30 $g.cm^{-2}.yr^{-1}$ (Figure 3). The highest MAR (~2.30 $g.cm^{-2}.yr^{-1}$) occur in the uppermost core section (post – 1990s), while the lowest values are found in the deeper, mid-20th century intervals. The parallel trends in sedimentation rate and MAR confirm that the observed variability reflects genuine changes in sediment flux to be seabed, rather than alterations in sediment density alone.

Temporal variability of Hg concentrations

Sedimentary mercury concentrations in core MD23-3660Q reveal a pronounced centennial-scale increase, with values rising from background levels to sustained historical highs (Figure 3A). Within the ^{210}Pb-dated interval (1916-2023), total Hg concentrations range from 44 to 118 ng g^{-1}. The lowest concentrations occur in the deeper part of the record, with progressive increase toward the surface.

Prior to the 1980s, Hg concentrations remained relatively stable and generally below 80 $ng.g^{-1}$. From the 1980s onward, a clear ascending trend is observed, with concentrations exceeding 100 $ng.g^{-1}$ in multiple intervals and peaking in the most recent sediments. This trend is not monotonic but is characterized by decadal-scale fluctuations superimposed on a long-term rise.

Critically, Hg levels throughout the entire MD23-3660Q record enriched relative to natural interglacial background conditions. Reference cores from the continental slope (MD23-3652Q, MD23-3653) show that pré-anthropogenic interglacial Hg concentrations peak at only ~30–32 $ng.g^{-1}$. Even the lowest concentrations in our shelf core the past century consistently surpass this natural baseline, indicating persistent anthropogenic influence.

The temporal pattern can be subdivided into three distinct phases (Figure 3A): Phase I (Early 1900 - ~ 1970s): Characterized by low, stable Hg concentrations (~44–80 ng g^{-1}). Phase II (~1980s - Early 2000s): Marked by increasing variability and a clear rise in concentrations, transitioning toward higher values. Phase III (Early 2000s - Present): Defined by consistently elevated concentrations, frequently > 100 ng.g^{-1}, representing the period of strongest Hg enrichment.

In summary, the sedimentary record documents a century of sustained enrichment above natural background levels, culminating in a period of accelerated accumulation since the early 2000s. This established trend proves the essential context for quantifying depositional fluxes and apportioning anthropogenic sources in the following analyses.

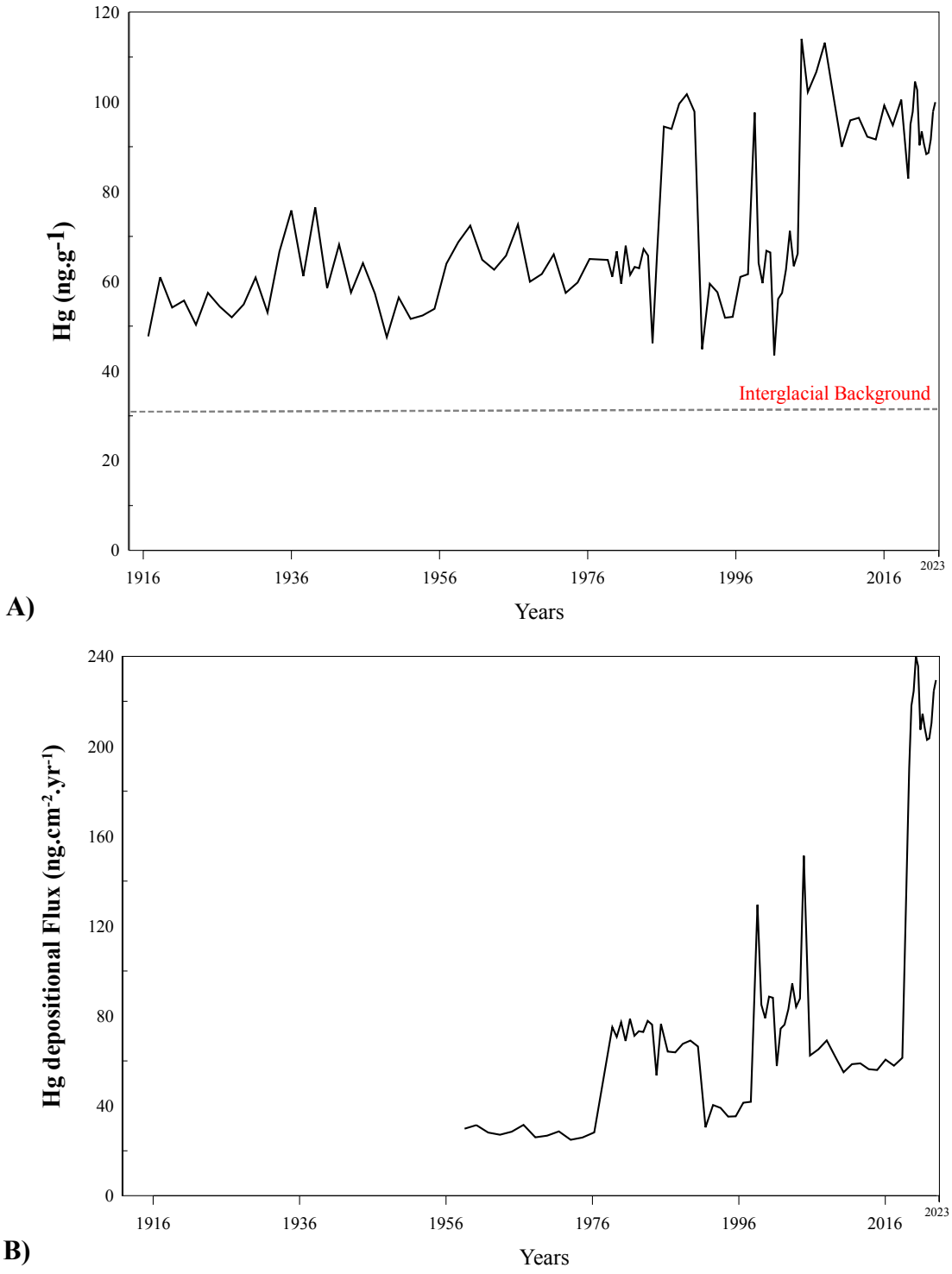

Figure 3: Mercury concentration and depositional flux over the last century in core MD23-3660Q. **(A)** Downcore Hg concentration profile (ng g^{-1}) compared to the natural interglacial background range (shaded area) derived from offshore reference cores MD23-3652Q and MD23-3653. All concentrations in the shelf core exceed pre-anthropogenic background levels. **(B)** Historical Hg depositional flux (ng cm^{-2} yr^{-1}), calculated as the product of Hg concentrations, sediment accumulation rate, and dry bulk density. The flux record highlights changes in the actual mass of Hg buried per unit area per year, providing a direct measure of anthropogenic forcing distinct from concentration variations driven by sediment dilution.

Hg depositional fluxes

Mercury depositional fluxes ($Flux_{Hg}$) for the ^{210}Pb-dated interval of core MD23-3660Q were calculated as the product of Hg concentrations, sedimentation rates, and dry bulk density (Figure 3B). Calculations were restricted to the upper 300.5 cm of the core, directly constrained by the chronology. The resulting $Flux_{Hg}$ record revels profound temporal variability over the past century, with a nearly order-of-magnitude increase from the mid-20th century to the present.

Long-term trend and phases. The record can be divided into distinct depositional phase based on flux magnitude: Phase I (~1960 - 1986), Characterized by relatively low and stable fluxes, ranging from ~25 to 32 ng cm $^{-2}$ yr $^{-1}$. This period reflects both low Hg concentrations and low sediment accumulation rates. Phase II (~1986 -1998), Fluxes increased to moderate levels (~30 - 70 ng cm $^{-2}$ yr $^{-1}$ with great variability, marking the initial departure from the earlier baseline. Phase III (~1999 - 2005). A period of marked increase, with fluxes reaching ~70 - 150 ng cm $^{-2}$ yr $^{-1}$. This rise was driven primarily by a pronounced spike in sediment accumulation rates, enhancing the delivery of moderately enriched Hg to the seabed. Phase IV (~2005 - 2019). Fluxes decreased to intermediate levels (~55 - 70 ng cm $^{-2}$ yr $^{-1}$), indicating a transient reduction in Hg burial efficiency. Phase V (~2019–2023). The most recent interval exhibits the highest fluxes in the record, exceeding 200 ng cm $^{-2}$ yr $^{-1}$ and peaking at approximately 230 ng.cm $^{-2}$.yr $^{-1}$. This maximum is driven by the synergistic combination of the highest Hg concentrations and the most rapid sediment accumulation observed in the core.

Overall, Hg burial on the Amazon Continental Shelf intensified dramatically over the study period, with modern fluxes approximately nine times greater than mid-20th century levels. This extreme variability underscores the dominance of non-steady-state depositional processes and provides the direct physical evidence necessary to attribute sources between regional and global drivers in the following analysis.

Global Hg Excess and Identification of Depositional Regimes

The sedimentary Hg record from the Amazon shelf shows an evolving relationship with global anthropogenic emissions, transitioning from broad covariance to marked regional divergence.

Local Hg concentrations show a significant long-term linear correlation with global atmospheric emission inventories (Pearson $r = 0.612$, $p < 0.0001$; Figure 4A). However, non-parametric rank correlations are weak and non-significant (Spearman $\rho = 0.429$, $p = 0.397$; Kendall $\tau = 0.200$, $p = 0.719$). This contrast reveals that while the overarching centennial trends a similar, the temporal trajectories are not monotonically aligned, indicating periods where local accumulation deviates from the global pace.

To isolate these deviations, we calculated Hg excess (Hg_{exc}) as the difference between Z-score normalized local and global records (Figure 4B). Positive Hg_{exc} denotes intervals when local accumulation outpaces the global atmospheric signal, signaling dominant regional forcing.

The Hg_{exc} record delineates three successive regimes:

1. Regime 1(~1916 - mid-1990s): Hg_{exc} fluctuates near zero, indicating that Hg burial on the shelf closely tracked the pace of global atmospheric emissions during this period.
2. Regime 2 (mid-1990s - early 2000s): The onset of sustained positive Hg_{exc} values a clear departure from the global trend, signifying the emergence of a significant regional Hg source.
3. Regime 3 (early 2000s - present): This period is characterized by the largest and most consistent positive Hgexc anomalies in the record, reflecting the unequivocal dominance over global Hg forcing in recent decades.

An Early Warning Signals (EWS) analysis based on rolling-window variance objectively identified two major breakpoints in the Hg_{exc} time series, centered at 1995 and 2004 (variance peaks >90th percentile; Figure 5). These breakpoints statistically validate the transition between the three depositional regimes described above.

The combined evidence from correlation analysis, Hg_{exc} calculations, and breakpoint detection demonstrates a fundamental reorganization record of Hg sources to the Amazon shelf. The system has shifted from a state modulated by global atmospheric emissions (Regime 1) to one overwhelmingly dominated by regional anthropogenic inputs (Regime 3), with a clear transitional phase (Regime 2). This quantitative framework provides robust evidence for the hypothesized North-to-South transition of Hg emissions, paving the way for investigating the specific regional drivers responsible for each regime.

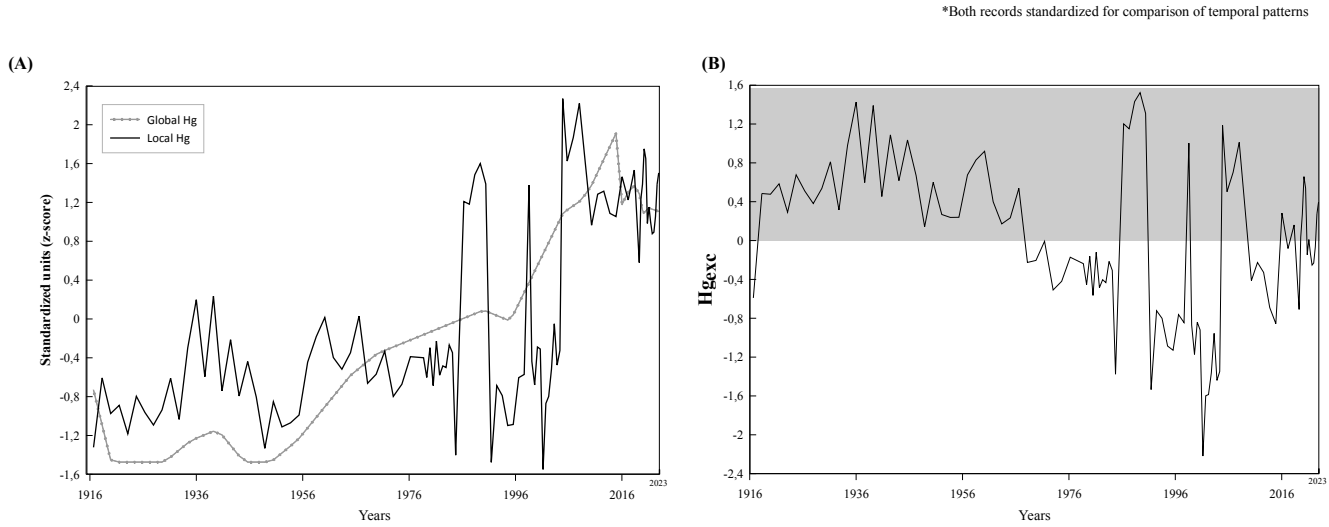

Figure 4: Disentangling global and regional sources. **(A)** Z-score standardized records of sedimentary Hg in core MD23-3660Q (local, blue) and Global Anthropogenic Atmospheric Emissions (GAAE, global, orange). The parallel long-term rise (pre-1990s) and subsequent divergence are visually apparent. **(B)** Mercury excess (Hg_{exc}), calculated as the difference between standardized records (local - global). Positive (Hg_{exc}) values (shaded) indicate periods when Hg accumulation on the Amazon shelf exceeded the trajectory of global atmospheric emissions, signaling the growing dominance of regional anthropogenic sources. The transition to sustained positive values after the mid-1990s marks a fundamental shift in the Hg source regime.

.

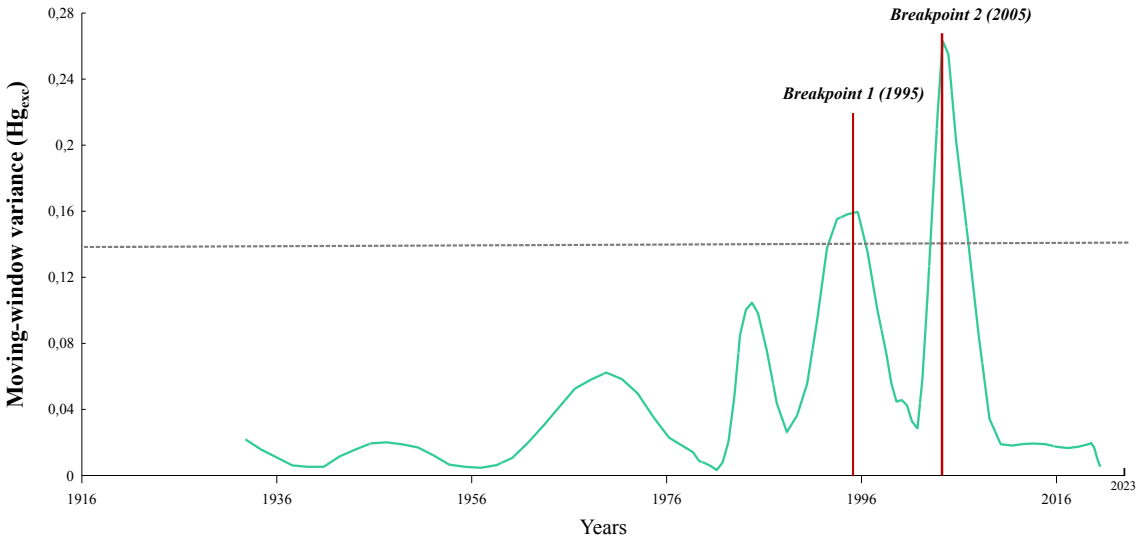

Figure 5: Statistical identification of depositional regime shifts. Early Warning Signals (EWS) analysis applied to Hg_{exc} time series, showing rolling-window variance. The horizontal dashed line indicates the 90th percentile significance threshold. Variance peaks exceeding this threshold identify two major breakpoints (~1995, ~ 2004), marked by vertical lines. These statistically derived breakpoints objectively validate the transition between the three Hg source regimes (global, transitional, regional) identified in the record, corroborating the shift from atmospheric to land-use dominated Hg forcing.

Geochemical associations and multivariate patterns

To investigate potential lithogenic or organic controls on Hg, we performed multivariate analysis on a suite of geochemical variables (major/ minor elements, TOC). Unsupervised K-means clustering of the full dataset identified a coherent subgroup representing sediments with moderate anthropogenic influence, which was isolated detailed analysis (Figure 6A).

Principal Component Analysis (PCA) on this subset yielded moderate cumulative variance explanation (67.7% for PC1+PC2; PC1=44.3%, PC2=23.4%), indicating the absence of a single, dominant geochemical gradient. Critically, Hg concentrations showed no significant correlation with either principal component (PC1: $r = 0.02$, $p = 0.87$; PC2: $r = 0.07$, $p = 0.57$). The loadings reveal that PC1 is broadly associated with a suite of lithogenic elements (Al, Si, K, Ti), While PC2 shows a modest relationship with TOC and Ca (Figure 6B). Notably, no single element exerts dominant influence, and Hg is not aligned with any major compositional axis.

We then tested whether Hg variability could be statistically predicted from the measured geochemical proxies. Both Random Forest and Partial Least Squares Regression (PLSR) models performed poorly, yielding strongly negative cross-validated R^2 values (-2.02 and −0.36, respectively). This consistent failure demonstrates that Hg concentrations cannot be reconstructed from the background lithogenic and organic sediment composition.

The weak geochemical coupling, diffuse PCA loadings, and failed predictive models collectively indicate that Hg accumulation on the Amazon Continental Shelf is not primarily controlled by natural sedimentary carriers (e.g., Fe-oxides, aluminosilicates, organic matter) or dilution processes. Instead, the decoupling of Hg from the local geochemical matrix provides strong, independent evidence that the observed enrichment is driven by external, anthropogenic inputs whose magnitude varies independently of the underlying sediment composition. This finding directly supports the attribution of the Hg excess (Hg_{exc}) to regional anthropogenic activities rather than to catchment weathering or oceanic biogeochemical processes.

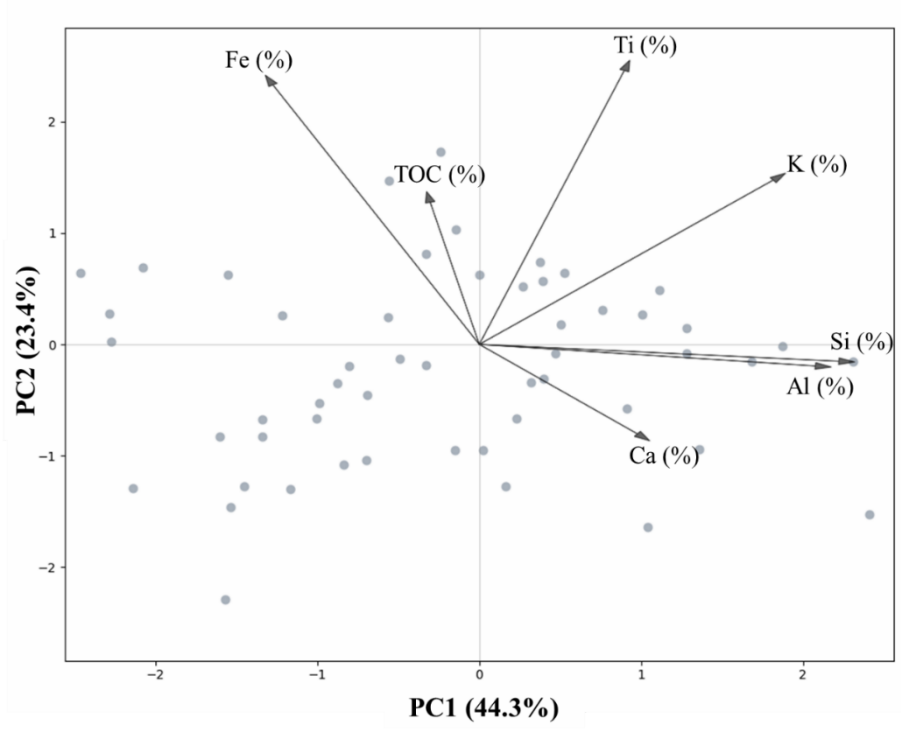

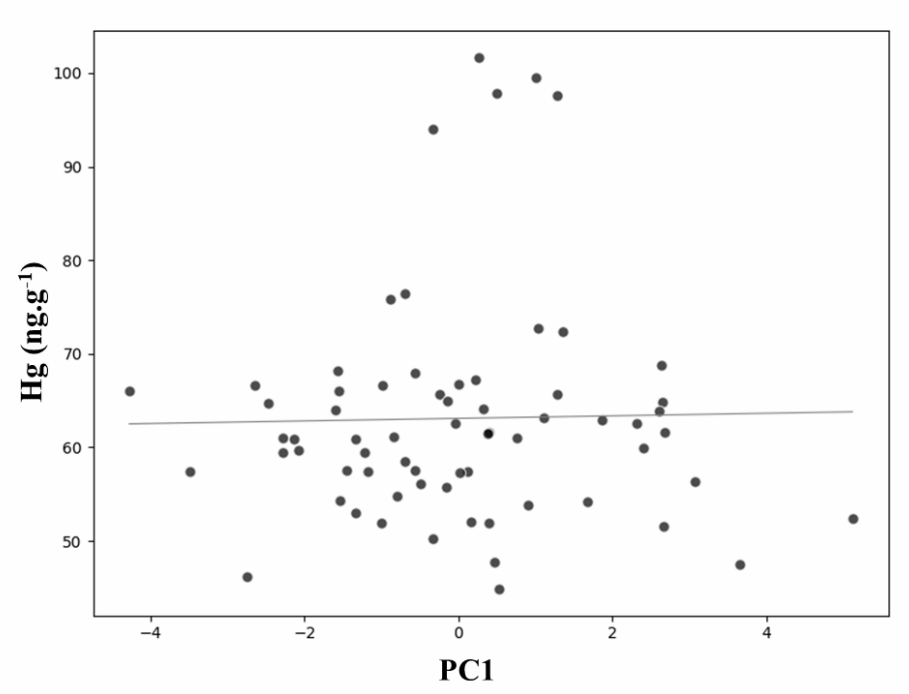

Figure 6: Decoupling of mercury from bulk sediment geochemistry. (A) Principal Component Analysis (PCA) biplot for sediments with moderate anthropogenic influence. The distribution of samples and variable loadings (vectors) on the first two components (PC1, PC2) reveals a dominant geochemical gradient aligned with Hg, which clusters near the origin (weak loadings). **(B)** Direct comparison of Hg concentrations against PC1 scores confirms the lack of a predictive relationship (r=0.02, p=0.87r=0.02, p=0.87). Together, these results demonstrate that Hg accumulation is not controlled by the major lithogenic or organic components of the sediment matrix, supporting its origin from external anthropogenic inputs.

Discussion

From global atmospheric forcing to regional dominance in Amazonian Hg deposition

The century-long-term mercury record at the Amazon River mouth encapsulates the evolving interplay between global and regional anthropogenic forcing. The significant linear correlation between local sedimentary Hg and Global Anthropogenic Atmospheric Emissions (GAAE) confirms that multi-decadal trends on the Amazon Continental Shelf (ACS) have historically covaries with global emission trajectories, (Figure 4A) (Streets et al., 2011; Obrist et al., 2018). This correspondence demonstrates that global atmospheric forcing provides an important background control, particularly during the early 20th century when industrial emissions in the Northern Hemisphere dominated the global mercury budget (Streets et al., 2011; Amos et al., 2014).

However, analysis of the standardized mercury excess record (Hg_{exc}) reveals that global forcing alone cannot explain the magnitude and temporal structure of Hg accumulation. While Hg_{exc} fluctuates around zero during the first half of the record, a sustained positive divergence emerges from the mid-1990s onward (Figure 4B), when local Hg accumulation increasingly exceeds expectations based on global atmospheric emissions alone. This marks a fundamental transition in the dominant controls on Hg deposition, from primarily global to regional drivers, consistent with the documented geographic redistribution of anthropogenic Hg emissions toward tropical regions (Obrist et al., 2018; Qiu et al., 2025).

The Early Warning Signals analysis further supports this interpretation by identifying statistically significant breakpoints centered around ~1995 and ~2004 (Figure 5). The breakpoints separate the record into three distinct depositional regimes and reflect changes in the statistical structure of Hg accumulation, indicating regime shifts in the way mercury was transferred and buried (Dakos et al., 2012; Scheffer et al., 2009). Importantly, these transitions are not synchronous with major inflections in global emission inventories, reinforcing the conclusion that regional processes became increasingly influential during the late 20th and early 21st centuries (Streets et al., 2011; Obrist et al., 2018).

At the global scale, rivers represent the largest pathway for mercury transfer from land to ocean (Liu et al., 2021). Within this context, the Amazon River system stands out as the single largest fluvial contributor worldwide, accounting for approximately 22% of global riverine Hg exports (Liu et al., 2021; Amos et al., 2014). This disproportionate contribution implies that changes in land-use practices and sediment mobilization within the Amazon basin can exert a first-order control on mercury delivery to the coastal ocean, rivaling or exceeding the influence of long-range atmospheric transport (Amos et al., 2014; Neupane et al., 2022).

The spatial concentration of artisanal and small-scale gold mining (ASGM) activities sin southeastern and southwestern sub-basins, particularly within the Madeira River watershed, suggests that Hg reaching the shelf sediments is predominantly mediated by fluvial transport and basin-scale redistribution (Lacerda and Salomons, 1992; Bastos et al., 2006).

Furthermore, the decoupling of Hg from bulk sediment geochemistry—evidenced by weak multivariate associations and the failure of predictive geochemical models (Figure 6)—provides independent evidence against a dominant lithogenic or organic carrier phase. This reinforces that the observed enrichment is driven by external, anthropogenic inputs whose flux is not governed by the underlying sediment composition.

Comparable interactions between global emissions and regional delivery have been documented in other systems (Engstrom et al., 2014; Yang et al., 2023; Kong et al., 2025). In the Amazon, however, the magnitude of the regional signal is particularly pronounced. The persistent increase in Hg concentrations above ~100 ng.g ^{1} since the early 2000s cannot be explained by global trends alone and instead points to a decisive regional contribution. Taken together, the Hg_{exc} record and the identification of discrete depositional regimes demonstrate that the ACS does not function as a passive archive of global atmospheric mercury. Rather, it acts as an active integrator where global forcing is increasingly modulated and, in recent decades, overridden by regional anthropogenic activities and basin-scale processes (Amos et al., 2014; Neupane et al., 2022).

Sedimentation as a key amplifier of mercury accumulation at the Amazon River mouth

The pronounced increase in mercury depositional fluxes observed in core MD23-3660Q cannot be attributed solely to of rising Hg concentrations but reflects the combined influence of contaminant availability and exceptionally high sediment accumulation rates (Figure 2). In large river-dominated margins, sedimentation acts as a primary physical control on contaminant burial (Allison et al., 1998; Liu et al., 2013). The Amazon Continental Shelf represents one of the most dynamic sedimentary environments globally, characterized by extreme variability in sediment supply and depositional processes (Nittrouer et al., 1995; Allison and Nittrouer, 2004).

Throughout the last century, Hg fluxes at the Amazon River mouth display variability spanning nearly an order of magnitude, closely tracking changes in sedimentation and mass accumulation rates rather than Hg concentrations alone (Figure 3B). Periods of enhanced Hg burial coincide with intervals of accelerated sediment accumulation, highlighting

sedimentation as a key amplifier. Similar relationships between contaminant fluxes and sediment delivery have been reported in other large river systems (Syvitski et al., 2005; Horowitz et al., 2014).

The Amazon River exports more than one billion tons of suspended sediments annually, sustaining an extensive sediment plume across the continental shelf (Nittrouer et al., 1995; Kineke et al., 1996). Within this plume, fine-grained particles enriched in iron and aluminum (oxy)hydroxides and organic matter provide highly effective sorption surfaces for Hg, promoting its particulate retention and subsequent burial (Gibbs, 1977; Garnier et al., 2025). As a result, relatively modest increases in Hg concentrations can translate into disproportionately large increases in depositional fluxes under conditions of elevated sediment supply (Figure 3C).

Temporal changes in sedimentation are driven by a combination of natural climatic variability and anthropogenic land-use disturbances. Variations in precipitation and climate modes such as ENSO influence sediment transport on interannual to decadal timescales (Molinier et al., 1996; Aalto et al., 2003). Superimposed on these natural drivers, widespread deforestation, and mining activities have enhanced soil erosion and sediment mobilization over recent decades (Coe et al., 2011; Gatti et al., 2014). These processes increase not only sediment delivery but also the mobilization of legacy Hg stored in soils, thereby reinforcing the coupling between sediment fluxes and Hg burial.

Comparisons with other continental margin settings further emphasize the unique role of sedimentation on the Amazon shelf. In many temperate coastal systems, lower sedimentation rates limit the magnitude of Hg fluxes despite elevated concentrations (Engstrom et al., 2014; Yang et al., 2023). In contrast, the Amazon shelf operates as a high-capacity sediment trap, where rapid burial can preserve short-term signals and amplify regional contaminant inputs (Allison et al., 2014; Walsh and Nittrouer, 2009). This amplification effect explains why Hg depositional fluxes increase more sharply than concentrations alone would suggest.

Importantly, the dominance of sedimentation as a control underscores that changes in Hg burial at the Amazon River mouth do not directly mirror atmospheric emission trends. Instead, physical transport processes act as a critical intermediary, translating basin-scale land-use change into the sedimentary record. This finding reinforces that the Amazon system functions not merely as a passive receiver but as an active processor in which sediment dynamics strongly regulate contaminant accumulation (Amos et al., 2014; Neupane et al., 2022).

The synergistic effects of shifting sources and intense sediment dynamics position the Amazon River mouth as a decisive hotspot in the modern Hg cycle. The transition to regional dominance, evidenced by the Hg_{exc} record and statistical breakpoints, means that local mitigation efforts (e.g., curbing ASGM, reducing deforestation) are now paramount for reducing Hg loads to the Atlantic Ocean. Simultaneously, the amplification by sedimentation implies that land-use policies affecting soil stability will have a direct and magnified impact on coastal Hg burial. This dual reality—a strong regional source signal coupled with a physically amplifying environment—underscores why global emission inventories and frameworks like the Minamata Convention must integrate land-use-driven Hg mobilization to accurately assess trends and efficacy in tropical systems.

Geochemical controls and the absence of a single dominant Hg carrier phase

geochemical analysis confirms that mercury accumulation on the Amazon shelf is not governed by a simple association with a single sedimentary phase, distinguishing it from many well-described temperate systems.

Principal Component Analysis (PCA) reveals that the first two components together explain only ~68% of the total variance, with no single axis exerting a dominant influence on Hg concentrations (Figure 6A). The dominant loadings on PC1 are associated with lithogenic elements (Al, Fe, Ti, K, Si, Ca), while total organic carbon exhibits only a modest covariance (Lacerda and Salomons, 1992; Mendes et al., 2016). Critically, mercury concentrations show weak and non-significant correlations with these principal components (Figure 6B). This diffuse geochemical signal indicates that Hg is distributed across mixed mineral–organic assemblages rather than being preferentially bound to a single, dominant carrier phase such as Fe-oxides or organic matter alone (Gibbs, 1977; Amos et al., 2014).

This apparent complexity is not an analytical failure but a defining feature of large, dynamic tropical river–ocean systems. Here, particle composition, hydrodynamic sorting, redox conditions, and diverse sediment sources interact over short spatiotemporal scales causing Hg partition among multiple phases, including mineral surfaces, organic coatings, and mixed aggregates

Predictive modeling approaches, including Random Forest and Partial Least Squares Regression, reinforce this interpretation by failing to produce robust explanatory relationships. The consistently poor predictive performance underscores that Hg variability

cannot be reduced to a small subset of geochemical predictors and reflects multidimensional controls not easily captured by standard statistical frameworks (Engstrom et al., 2014; Yang et al., 2023). Comparable limitations have been reported in other complex coastal environments where physical and geochemical processes interact (Amos et al., 2014; Obrist et al., 2018).

In the Amazon, this complexity is amplified by immense transport and diversity provenance from different tributaries and land-use zones, introducing heterogeneity that influences Hg partitioning (Amos et al., 2014; Neupane et al., 2022). Consequently, the very absence of a strong geochemical control provides positive evidence for an external, anthropogenic Hg source whose input is decoupled from the natural lithogenic and organic sediment matrix.

Taken together, these results indicate that Hg accumulation at the Amazon River mouth is governed by diffuse, system-level controls. This finding cautions against the direct application of proxy-based or model-driven approaches developed for simpler systems when interpreting sedimentary Hg records in large tropical deltas (Obrist et al., 2018; Kong et al., 2025).

Implications for monitoring tropical Hg dynamics under the Minamata Convention

The Minamata Convention on Mercury represents a landmark global effort to reduce anthropogenic Hg emissions. However, its effectiveness relies a robust observational baseline capable of capturing both global trends and regionally driven responses (UNEP, 2019; Obrist et al., 2018). Sedimentary archives from large tropical river–ocean systems like the Amazon remain critically underrepresented in global monitoring, despite their unique capacity to integrate atmospheric, fluvial, and land-use-driven Hg inputs over policy-relevant timescales.

Our results demonstrate a clear divergence between global atmospheric emission inventories and local sedimentary Hg accumulation since the mid-1990s. This decoupling reveals a critical limitation: reductions in long-range atmospheric emissions achieved in the Global North may not translate into proportional declines in Hg burial within tropical regions, where basin-scale processes (deforestation, ASGM, erosion) can dominate and amplify Hg mobilization (Amos et al., 2014; Qiu et al., 2025).

Large tropical rivers play a disproportionate role in the global mercury cycle. The Amazon system alone contributes a significant fraction of global riverine Hg fluxes,

positioning its continental shelf as a critical interface (Liu et al., 2021). Sediment cores from this setting therefore provide an integrative archive that complements atmospheric data, offering essential insights into how global policy is modulated by regional environmental processes.

Therefore, evaluations of the Minamata Convention would benefit substantially from incorporation sediment-based indicators in tropical regions. Such records are vital for detecting delayed responses, indirect effects, and emerging regional sources not fully captured by national reporting mechanisms or atmospheric networks (Obrist et al., 2018; Neupane et al., 2022). The Amazon River mouth exemplifies a strategic sentinel site for tracking the Anthropocene's evolving balance between global and regional Hg forcing.

While this study stablishes a crucial century-scale baseline, challenges remain-spatial heterogeneity across the shelf, unquantified ASGM activity, and the future climate impacts on hydrology all warrant further investigation. Expanding high-resolution sedimentary monitoring across tropical margins is not merely supplementary but essential for refining global Hg budgets robustly assessing the long-term efficacy of the Minamata Convention (UNEP, 2019; Qiu et al., 2025). As the locus of anthropogenic Hg emissions shifts decisively toward the tropics, the river mouths of these systems must be recognized as ground-zero for monitoring the success of global mitigation efforts.

Conclusions

This study provides the first century-scale reconstruction of mercury accumulation at the mouth of the world's largest river, revealing a fundamental reorganization of Hg sources to the Amazon Continental Shelf. While the sedimentary record initially tracks global anthropogenic emission trends, a pronounced divergence emerges from the mid-1990s onward, making a decisive transition from global atmospheric forcing to regional dominance.

The mercury excess (Hg_{exc}) record and statistically validated regime shifts demonstrate that recent Hg burial cannot be explained by global atmospheric emissions alone. Instead, the acceleration of Artisanal and Small-scale Gold Mining (ASGM), widespread deforestation, and associated soil erosion across the Amazon Basin have become the dominant drivers of Hg mobilization. This regional signal is powerfully amplified by the system's exceptional sediment dynamics, where high sediment loads and variable accumulation rates enhanced particulate Hg burial, leading to a ninefold increase in depositional fluxes over.

Multivariate geochemical analyses confirm that Hg in this setting is not controlled by a single dominant carrier phase but by diffuse, multidimensional interactions within a complex sedimentary matrix. This intrinsic complexity, characteristic of large tropical river–ocean interfaces, challenges the application of simplified geochemical proxies developed for more stable environments.

Collectively, these findings establish that the Amazon River mouth acts as an active integrator and net accumulator of regionally sourced Hg, rather than a passive archive of global emissions. The transition documented here-from global atmospheric to regional land-use dominance-positions tropical river mouths as critical sentinels for tracking the anthropogenic reorganization of the global mercury cycle. Our results underscore the urgent need to incorporate land-use driven Hg mobilization and sedimentary fluxes into global emission inventories and the monitoring framework of the Minamata Convention to accurately assess the effectiveness of mitigation efforts in rapidly changing tropics.

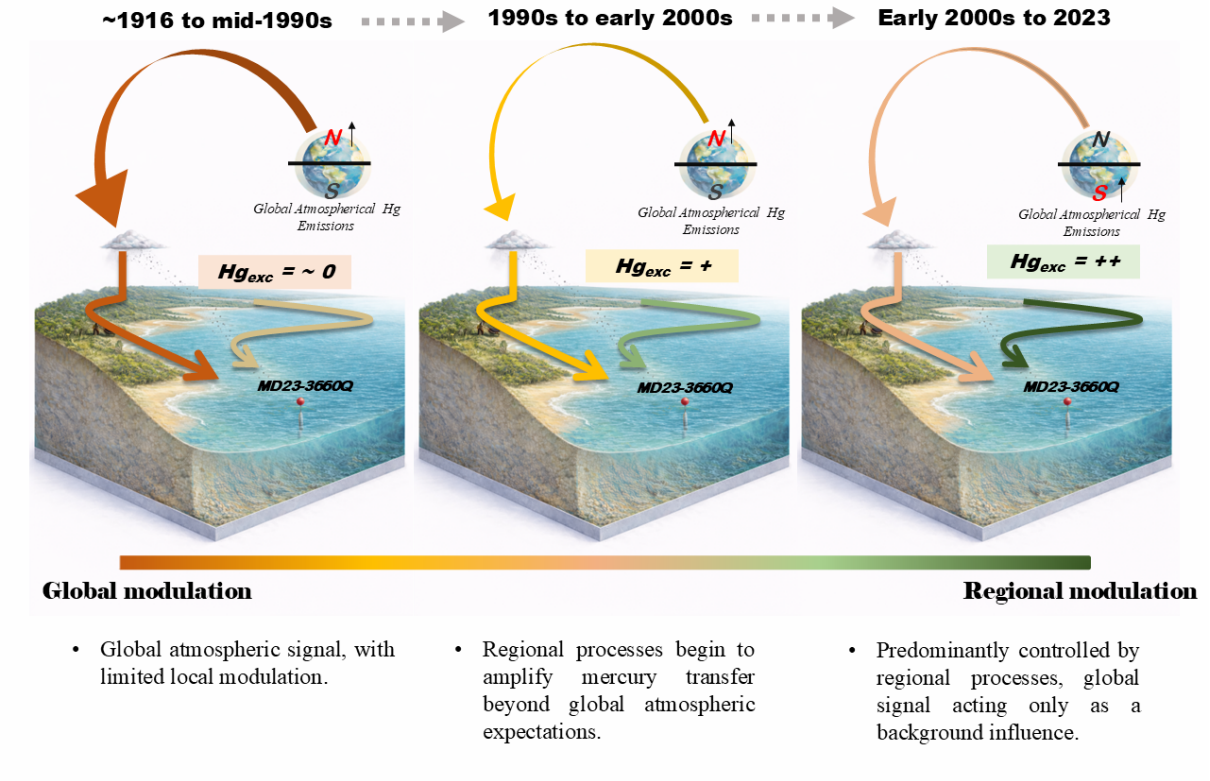

Figure 7: Conceptual model of mercury source transition and amplification at the Amazon River mouth. The model synthesizes the key drivers of Hg accumulation over the past century, derived from the sedimentary record of core *MD23-3660Q*. It depicts a temporal transition from a Global Atmospheric Regime (pre – 1990s), where Hg deposition tracked worldwide emission trends, to a Regional Anthropogenic Regime (post – 1990s), dominated by inputs from artisanal gold mining (ASGM) and land-use change (e.g., deforestation). This regional signal is physically amplified by the Amazon's exceptionally high sediment loads and variable sedimentation rates, leading to disproportionate increases in Hg burial fluxes. The Amazon Continental Shelf functions as an integrator and a sentinel system, providing a critical sedimentary baseline for monitoring the effectiveness of global agreements like the Minamata Convention in the tropics.

By establishing a high-resolution, century-scale sedimentary baseline in the world's largest tropical system, this study underscores the critical importance of incorporating sediment archives from river-dominated margins into global mercury assessments. Such records are essential for evaluating how international mitigation efforts, particularly under the Minamata Convention, translated into tangible environmental responses, especially in tropical regions where land-use change can override global atmospheric trends. Consequently, the Amazon Continental Shelf emerges as a pivotal sentinel site for monitoring the evolving balance between global policies and regional anthropogenic pressures on the mercury cycle in the Anthropocene.

References

Agência Nacional de Mineração (ANM). 2024. *Brazilian Mineral Summary 2024 – Iron (base year 2023)*. ANM, Brasília.

Albuquerque, P. T., Frédou, T., Arruda, G. N., Filho, C. A. S., Nascimento, A. F., da Silva, M. J., & De França, E. J. (2019). Tracking Hg historical inputs by Pb-210 geochronology for the Itapessoca estuarine complex, Pernambuco, Brazil. Journal of Radioanalytical and Nuclear Chemistry, 321(3), 875-883.

Allison, M. A., Nittrouer, C. A., & Faria Jr, L. D. C. (1995). Rates and mechanisms of shoreface progradation and retreat downdrift of the Amazon River mouth. *Marine Geology*, *125*(3-4), 373-392.

Amos, H. M., Jacob, D. J., Kocman, D., Horowitz, H. M., Zhang, Y., Dutkiewicz, S., ... & Sunderland, E. M. (2014). Global biogeochemical implications of mercury discharges from rivers and sediment burial. *Environmental science & technology*, *48*(16), 9514-9522.

Aula, I., Braunschweiler, H., & Malin, I. (1995). The watershed flux of mercury examined with indicators in the Tucurui reservoir in Para, Brazil. Science of the total environment, 175(2), 97-107.

AZEVEDO, F. A. Toxicologia do mercúrio. São Paulo: RIMA, 2003.

Barbosa, L.; Lobato, A. L.; Drummond. J. A. Garimpo, meio ambiente e sociedades indígenas. EDUFF. Niterói – RJ. CETEM – Centro de Tecnologia Mineral. 1992.

Bastos, W. R., Gomes, J. P. O., Oliveira, R. C., Almeida, R., Nascimento, E. L., Bernardi, J. V. E., ... & Pfeiffer, W. C. (2006). Mercury in the environment and riverside population in the Madeira River Basin, Amazon, Brazil. Science of the Total environment, 368(1), 344-351.

Bi, Q., Lv, S., He, Q., Liu, X., Zhou, L., Zheng, X., & Wang, Y. (2024). Analysis of mercury fractions in the fine grains of surface sediments in the Changjiang Estuary wetlands using thermodesorption and chemical extraction methods. *Journal of Soils and Sediments*, *24*(10), 3507-3514.

Bisinoti, M. C., Sargentini Júnior, É., & Jardim, W. F. (2007). Seasonal behavior of mercury species in waters and sediments from the Negro River Basin, Amazon, Brazil. Journal of the Brazilian Chemical Society, 18, 544-553.

BONOTTO, Daniel Marcos; VERGOTTI, Marcelo. 210Pb and compositional data of sediments from Rondonian lakes, Madeira River basin, Brazil. Applied Radiation and Isotopes, v. 99, p. 5-19, 2015.

Bouchez, J., F. Métivier, M. Lupker, L. Maurice, M. A. Perez,and C. France Lanord (2010), Prediction of depth integratedfluxes of suspended sediment in the Amazon River: Particleaggregation as a complicating factor, Hydrol. Processes, 25,778–794, doi:10.1002/hyp.7868

BOUCHEZ, Julien et al. Grain size control of river suspended sediment geochemistry: Clues from Amazon River depth profiles. **Geochemistry, Geophysics, Geosystems**, v. 12, n. 3, 2011.

BROWN, Kendall W. Colonial andean silver, the global economy, and indigenous labour in Peru's Huancavelica Mercury Mines of Death. The Extractive Industries and Society, v. 3, n. 3, p. 762-771, 2016.

CARNEIRO, Marcelo Sampaio; MANCINI, Roberto Martins. O desenvolvimento da produção siderúrgica na Amazônia Oriental e o debate sobre o processo de aprimoramento tecnológico e social. Estudos de Sociologia, p. e023015-e023015, 2023.

Casagrande, G. C. R., Dambros, J., De Andrade, E. A., Martello, F., Sobral-Souza, T., Moreno, M. I. C., ... & De Andrade, R. L. T. (2023). Atmospheric mercury in forests: accumulation analysis in a gold mining area in the southern Amazon, Brazil. *Environmental Monitoring and Assessment*, *195*(4), 477.

Castro, N. S. S. D., Braga, C. M., Trindade, P. A. D. A., Giarrizzo, T., & Lima, M. D. O. (2016). Mercury in fish and sediment of Purus River, Acre State, Amazon. Cadernos Saúde Coletiva, 24(3), 294-300.

Chede, B. S., Venancio, I. M., Figueiredo, T. S., Albuquerque, A. L. S., & Silva-Filho, E. V. (2022). Mercury deposition in the western tropical South Atlantic during the last 70 ka. *Palaeogeography, Palaeoclimatology, Palaeoecology*, *601*, 111122.

Chen, L., Liu, C., Yin, Y., Liu, G., Li, Y., & Cai, Y. (2022). Mass budget of mercury (Hg) in the seawater of Eastern China Marginal Seas: importance of the sediment–water transport processes. *Environmental Science & Technology*, *56*(16), 11418-11428.

Corbitt, E. S., Jacob, D. J., Holmes, C. D., Streets, D. G., & Sunderland, E. M. (2011). Global source–receptor relationships for mercury deposition under present-day and 2050 emissions scenarios. *Environmental science & technology*, *45*(24), 10477-10484.

Cortinhas Ferreira Neto, L., Diniz, C. G., Maretto, R. V., Persello, C., Silva Pinheiro, M. L., Castro, M. C., ... & Klautau, A. (2024). Uncontrolled illegal mining and Garimpo in the Brazilian Amazon. *Nature communications*, *15*(1), 9847.

Crizanto, J. L. P., de Abreu, C. H. M., de Souza, E. B., & da Cunha, A. C. (2024). Modeling the Impacts of Sea Level Rise Scenarios on the Amazon River Estuary. *Hydrology*, *11*(6), 86.

Dastoor, A., Wilson, S. J., Travnikov, O., Ryjkov, A., Angot, H., Christensen, J. H., ... & Muntean, M. (2022). Arctic atmospheric mercury: Sources and changes. *Science of The Total Environment*, *839*, 156213.

De Castro Paiva, T., Pestana, I. A., de Oliveira, B. C. V., Malm, O., de Rezende, C. E., & Kasper, D. (2024). Temporal variation of mercury levels in fish, soil, and sediments in an Amazon reservoir: insights from 35 years of river impoundment in Pará State, Brazil. Environmental Monitoring and Assessment, 196(11), 1089.

de Freitas, P. P., Cirano, M., Teixeira, C. E. P., Melres, S. J. R., Gomes, V. J. C., Guerrero-Martin, C. A., & Koch-Larrouy, A. (2025). Spatial and temporal variability of hydrodynamics on the Amazon Continental Shelf: an observational approach. *Continental Shelf Research*, 105491.

Do Nascimento, L. S., Pestana, I. A., Seidel, M., da Silva Junior, J. M., de Oliveira, B. C. V., Gomes, P. R., ... & de Rezende, C. E. (2025). Mercury concentrations along the Amazon estuary and plume: Spatial trends and geochemical processes. Environmental Research, 271, 121129.

Dukat, D.A., Kuehl, S.A., 1995. Non-steady-state 210Pb flux and the use of 228Ra/226Ra as a geochronometer on the Amazon continental shelf. Mar. Geol. 125, 329e350.

Engstrom, D. R., Fitzgerald, W. F., Cooke, C. A., Lamborg, C. H., Drevnick, P. E., Swain, E. B., ... & Balcom, P. H. (2014). Atmospheric Hg emissions from preindustrial gold and silver extraction in the Americas: A reevaluation from lake-sediment archives. *Environmental science & technology*, *48*(12), 6533-6543.

Fadina, O. A., Venancio, I. M., Belem, A., Silveira, C. S., de Castro Bertagnolli, D., Silva-Filho, E. V., & Albuquerque, A. L. S. (2019). Paleoclimatic controls on mercury deposition in northeast Brazil since the Last Interglacial. *Quaternary Science Reviews*, *221*, 105869.

FARO, L. C.; POUSA, C.; Fernandez, C. Conversas com Eliezer. Rio de Janeiro: Insight Engenharia de Comunicação, 2005.

FERREIRA, Victor Rennan Santos et al. Amazon streams impacted by bauxite mining present distinct local contributions to the beta diversity of aquatic insects, fish, and macrophytes. Science of The Total Environment, v. 955, p. 177292, 2024.

Figueiredo, T. S., Santos, T. P., Costa, K. B., Toledo, F., Albuquerque, A. L. S., Smoak, J. M., ... & Silva-Filho, E. V. (2020). Effect of deep Southwestern Subtropical Atlantic Ocean circulation on the biogeochemistry of mercury during the last two glacial/interglacial cycles. *Quaternary Science Reviews*, *239*, 106368.

Fisher, J. A., Schneider, L., Fostier, A. H., Guerrero, S., Guimarães, J. R. D., Labuschagne, C., ... & Walters, C. (2023). A synthesis of mercury research in the Southern Hemisphere, part 2: Anthropogenic perturbations. *Ambio*, *52*(5), 918-937.

Garnier, J., Martin, L. A., Sonke, J. E., Souza, J., Quintarelli, J., Kutter, V., ... & Seyler, P. (2025). Mercury isotope constraints on artisanal and small-scale gold mining source contributions and redox cycling in the Yanomami Indigenous Territory. Journal of Hazardous Materials, 139892.

HORTELLANI, Marcos Antonio et al. Evaluation of mercury contamination in sediments from Santos-São Vicente estuarine system, São Paulo state, Brazil. **Journal of the Brazilian Chemical Society**, v. 16, p. 1140-1149, 2005.

Ignatavičius, G., Unsal, M. H., Busher, P., Wołkowicz, S., Satkūnas, J., Šulijienė, G., & Valskys, V. (2022). Geochemistry of mercury in soils and water sediments. *AIMS environmental science.*, *9*(3), 261-281.

Jaeger, J.M., Nittrouer, C.A., 1995. Tidal controls on the formation of fine-scale sedimentary strata near the Amazon River mouth. Mar. Geol. 125, 259e281

Kong, X., Zhang, J., Liu, Q., Li, Y., & He, Q. (2025). Cascading tipping points of mercury dynamics in coastal sediments: Anthropogenic-enhanced deposition vs. warming-driven remobilization. *Environmental Pollution*, 127130.

Kuehl, S.A., Nittrouer, C.A., Allison, M.A., Faria, L.E.C., Dukat, D.A., Jaeger, J.M., Pacioni, T.D., Figueiredo, A.G., Underkoffler, E.C., 1996. Sediment deposition, accumulation, and seabed dynamics in an energetic fine-grained coastal environment. Cont. Shelf Res. 16 (5/6), 787e815.

Kuehl, S.A., Pacioni, T.D., Rine, J.M., 1995. Seabed dynamics of the inner Amazon continental shelf: temporal and spatial variability of surficial strata. Mar. Geol. 125, 283e302.

KUEHL, Steven A. et al. An overview of sedimentation on the Amazon continental shelf. **Geo-marine letters**, v. 4, n. 3, p. 207-210, 1984.

Lacerda, L. D., Pfeiffer, W. C., Malm, O., Souza, C. M. M., Bastos, W. R., and Silveira, E. G. 1987. Contaminação por mercurio na Amazônia: análise preliminar do Rio Madeira, RO. Anais do I Congresso Brasileiro Geoquimica, 2: 295-299.

LACERDA, Luiz Drude de; SALOMONS, Win. **Mercúrio na Amazônia: uma bomba relógio química?**. CETEM, 1992.

LACERDA, Luiz Drude; DE ALMEIDA, Ronaldo; BASTOS, Wanderley Rodrigues. A 35-year record (1987–2022) of Hg concentrations in two of the fish species most consumed by people living in the upper Madeira River Basin, Brazilian Amazon region. **Toxics**, v. 12, n. 2, p. 144, 2024.

LACERDA, Luiz. Updating global Hg emissions from small-scale gold mining and assessing its environmental impacts. **Environmental Geology**, v. 43, n. 3, p. 308-314, 2003.

Lechler, P. J., Miller, J. R., Lacerda, L. D. D., Vinson, D., Bonzongo, J. C., Lyons, W. B., & Warwick, J. J. (2000). Elevated mercury concentrations in soils, sediments, water, and fish of the Madeira River basin, Brazilian Amazon: a function of natural enrichments?. Science of the Total Environment, 260(1-3), 87-96.

Lino, A. S., Kasper, D., Guida, Y. S., Thomaz, J. R., & Malm, O. (2019). Total and methyl mercury distribution in water, sediment, plankton and fish along the Tapajós River basin in the Brazilian Amazon. Chemosphere, 235, 690-700.

Liu, L., Wang, J., Wang, L., Hu, Y., & Ma, X. (2019). Vertical distributions of mercury in marine sediment cores from central and southern part of Bohai Sea, China. Ecotoxicology and environmental safety, 170, 399-406.

Liu, M., Zhang, Q., Maavara, T., Liu, S., Wang, X., & Raymond, P. A. (2021). Rivers as the largest source of mercury to coastal oceans worldwide. *Nature Geoscience*, *14*(9), 672-677.

Liu, Z., Pan, S., Yin, Y., Ma, R., Gao, J., Xia, F., & Yang, X. (2013). Reconstruction of the historical deposition environment from 210Pb and 137Cs records at two tidal flats in China. Ecological engineering, 61, 303-315.

MACHADO, Raymundo de Campos. Apontamentos da história do alumínio primário no Brasil. Ouro Preto: Fundação Gorceix, 1985.

Machado, W., Santelli, R. E., Loureiro, D. D., Oliveira, E. P., Borges, A. C., Ma, V. K., & Lacerda, L. D. (2008). Mercury accumulation in sediments along an eutrophication gradient in Guanabara Bay, Southeast Brazil. *Journal of the Brazilian Chemical Society*, *19*, 569-575.

MASON, R. P.; FITZGERALD, W. F.; MOREL, F. M. M. The biogeochemical cycling of elemental mercury - anthropogenic influences. Geochim. Cosmochim. Acta, London, v. 58, n.15, p. 3191 – 3198, 1994.

Mendes, L. A., de Lena, J. C., do Valle, C. M., Fleming, P. M., & Windmöller, C. C. (2016). Quantification of methylmercury and geochemistry of mercury in sediments from a contaminated area of Descoberto (MG), Brazil. *Applied Geochemistry*, *75*, 32-43.

Moore, W.S., DeMaster, D.J., Smoak, J.M., McKee, B.A., Swarzenski, P.W., 1996. Radionuclide tracers of sedimentewater interactions on the Amazon shelf. Cont. Shelf Res. 16 (5/6), 645e665.

Morozov, E. G., Frey, D. I., Salyuk, P. A., & Budyansky, M. V. (2024). Amazon River Plume in the Western Tropical North Atlantic. *Journal of Marine Science and Engineering*, *12*(6), 851.

NERY, José Reinaldo Cardoso; BONOTTO, Daniel Marcos. 210Pb and composition data of near-surface sediments and interstitial waters evidencing anthropogenic inputs in Amazon River mouth, Macapá, Brazil. **Journal of Environmental Radioactivity**, v. 102, n. 4, p. 348-362, 2011.

Neupane, B., Bao, K., Chen, M., Thapa, P., & Meadows, M. E. (2022). The timing and magnitude of anthropogenic mercury pollution: A 200-year record from multi-lake sediment cores in northeast China. *Chemosphere*, *309*, 136803.

Nittrouer, C. A., DeMaster, D. J., Kuehl, S. A., Figueiredo Jr, A. G., Sternberg, R. W., Faria, L. E. C., ... & Fricke, A. T. (2021). Amazon sediment transport and accumulation along the continuum of mixed fluvial and marine processes. *Annual Review of Marine Science*, *13*(1), 501-536.

Obrist, D., Kirk, J. L., Zhang, L., Sunderland, E. M., Jiskra, M., & Selin, N. E. (2018). A review of global environmental mercury processes in response to human and natural perturbations: Changes of emissions, climate, and land use. *Ambio*, *47*(2), 116-140.

OLIVEIRA, Marcus PA; FERREIRA, Rodrigo L. Extending beyond individual caves: a graph theory approach broadening conservation priorities in Amazon iron ore caves. PeerJ, v. 12, p. e16877, 2024.

Oliveri, E., Manta, D. S., Bonsignore, M., Cappello, S., Tranchida, G., Bagnato, E., ... & Sprovieri, M. (2016). Mobility of mercury in contaminated marine sediments: biogeochemical pathways. *Marine Chemistry*, *186*, 1-10.

OLIVIER, Léa et al. Late summer northwestward Amazon plume pathway under the action of the North Brazil Current rings. **Remote Sensing of Environment**, v. 307, p. 114165, 2024.

PADBERG, S. (1990). Mercury determination in samples from Tapajós river (Itaituba), lnstitut for Angewandte Physikalische Chemie ICH-4. *Forschungszeutren Jullich Jullich D-5170, 13p*.

Pfeiffer, W. C. (1988). Drude de Lacerda L. Mercury inputs into the Amazon Region, Brazil. *Environ Technol Lett*, *9*, 325-330.

PFEIFFER, W. C. et al. Environmental fate of mercury from gold mining in the Brazilian Amazon. **Environmental Reviews**, v. 1, n. 1, p. 26-37, 1993.

Qiu, X., Liu, M., Zhang, Y., Zhang, Q., Lin, H., Cai, X., ... & Tao, S. (2025). Declines in anthropogenic mercury emissions in the Global North and China offset by the Global South. *Nature Communications*, *16*(1), 1179.

Sanei, H., Outridge, P. M., Oguri, K., Stern, G. A., Thamdrup, B., Wenzhöfer, F., ... & Glud, R. N. (2021). High mercury accumulation in deep-ocean hadal sediments. *Scientific reports*, *11*(1), 10970.

Santos, D. C., Souza-Filho, P. W. M. D., Nascimento Júnior, W. D. R., Crósta, Á. P., & Lopes, J. P. Land Use Changes and Iron Ore Production in Open Pit Mines of Brazil from 1984 to 2019: An Indicator of Land Use Intensity. *Available at SSRN 4569411*.

SIQUEIRA, Gilmar W.; APRILE, Fabio M. Distribuição de mercúrio total em sedimentos da plataforma continental Amazônica: Brasil. Acta Amazonica, Manaus, v. 42, n. 2, p. 259-268, jun. 2012. DOI: http://dx.doi.org/10.1590/S0044-59672012000200012.

Smoak, J.M., DeMaster, D.J., Kuehl, S.A., Pope, R.H., McKee, B.A., 1996. The behavior of particle-reactive tracers in a high turbidity environment: 234Th and 210Pb on the Amazon continental shelf. Geochim. Cosmochim. Acta 60 (12), 2123e2137

SOUZA, Rikelly Souza et al. Bauxite mining in the Amazon: impacts of environmental recovery methods on soil organic matter and physical attributes. Landscape and Ecological Engineering, v. 21, n. 4, p. 745-756, 2025.

Streets, D. G., Devane, M. K., Lu, Z., Bond, T. C., Sunderland, E. M., & Jacob, D. J. (2011). All-time releases of mercury to the atmosphere from human activities. *Environmental science & technology*, *45*(24), 10485-10491.

Telmer, K., Costa, M., Angélica, R. S., Araujo, E. S., & Maurice, Y. (2006). The source and fate of sediment and mercury in the Tapajós River, Pará, Brazilian Amazon: Ground-and space-based evidence. Journal of environmental management, 81(2), 101-113.

TRINDADE, Roberto de Barros Emery; BARBOSA FILHO, Olavo (ed.). **Extração de ouro**: princípios, tecnologia e meio ambiente. Rio de Janeiro: CETEM - Centro de Tecnologia Mineral, 2002.

Van Schaik, E., Killaars, L., Smith, N. E., Koren, G., Van Beek, L. P. H., Peters, W., & van der Laan-Luijkx, I. T. (2018). Changes in surface hydrology, soil moisture and gross primary production in the Amazon during the 2015/2016 El Niño. *Philosophical Transactions of the Royal Society B: Biological Sciences*, *373*(1760), 20180084.

West, T. A., & Fearnside, P. M. (2021). Brazil's conservation reform and the reduction of deforestation in Amazonia. *Land use policy*, *100*, 105072.

Yang, H., Macario-González, L., Cohuo, S., Whitmore, T. J., Salgado, J., Peréz, L., ... & O'Dea, A. (2023). Mercury pollution history in tropical and subtropical American lakes: multiple impacts and the possible relationship with climate change. *Environmental Science & Technology*, *57*(9), 3680-3690.